


Comparison of WaPOR RS-based to SWAT+ model water productivity estimates in Lake Naivasha Basin, Kenya.

HELLEN VIVIAN KHATUNDI WANJALA
July, 2020

SUPERVISORS:
Dr. Ir. C.M.M. Mannaerts
Dr. B.H.P. Maathuis

ADVISOR:
Ir. H.F. Benninga



Comparison of WaPOR RS-based to SWAT+ model water productivity estimates in Lake Naivasha Basin, Kenya.

HELLEN VIVIAN KHATUNDI WANJALA
Enschede, The Netherlands, July, 2020.

Thesis submitted to the Faculty of Geo-Information Science and Earth Observation of the University of Twente in partial fulfilment of the requirements for the degree of Master of Science in Geo-information Science and Earth Observation.
Specialization: Water Resources and Environmental Management

SUPERVISORS:
Dr. Ir. C.M.M. Mannaerts
Dr. B.H.P. Maathuis

ADVISOR:
Ir. H.F. Benninga

THESIS ASSESSMENT BOARD:
Dr. Ir. M.W. Lubczynski (Chair)
Mrs. A. Klaasse MSc (External Examiner, eleaf, Wageningen)

DISCLAIMER

This document describes work undertaken as part of a programme of study at the Faculty of Geo-Information Science and Earth Observation of the University of Twente. All views and opinions expressed therein remain the sole responsibility of the author, and do not necessarily represent those of the Faculty.

ABSTRACT

Many countries face challenges in the water and food sector, especially with the current rapid population growth, and increasing water scarcity due to climate change. Policies and actions have been implemented in order to meet these demands. Kenya is among these countries, and applies various policies to boost the land and water productivity in agriculture; crop or livestock, forestry, fisheries and more. The slogan 'more food per drop' is often used.

Water productivity (WP) refers to the ratio of mass of agricultural output to the amount of water consumed. Different approaches have been adopted in measuring WP. Food and Agriculture Organization, the United Nations (FAO-UN) plays a leading role in this with the Water Productivity Open-access portal of Remotely-sensed data (WaPOR) that provides land and water productivity information across Africa and the Near East.

To ensure that WaPOR datasets are efficient to users, quality assessment via validation and comparative analyses have been (and are still) conducted on different WP data components. This research compares WaPOR level II to SWAT+ model WP estimates in the Lake Naivasha basin located in the Rift Valley in Kenya, over an 11 years period (2009-2019). SWAT+, which is a new version of the SWAT model, is a physical-based, semi-distributed hydrological model that performs simulations on crop growth, hydrological balance (surface and groundwater), water quality, and sediment transportation in a catchment.

Fieldwork was first conducted, on 8-25th January 2020, with an aim to collect ground-truth information on the land cover, and crop phenological information with the basic land and water management practices from farmers in the catchment. The SWAT+ model for the Lake Naivasha basin was then established to simulate total biomass production and actual evapotranspiration, after which the WP estimates from SWAT+ could be calculated. These were then compared to the WaPOR WP estimates. As the nature of the datasets from these two approaches is different, only the long term average results were compared.

Average annual TBP and ETa values of 23723.5 kg/ha/year and 823.6 mm/year, and 31974.7 kg/ha/year and 800.2 mm/year from WaPOR and SWAT+ respectively were obtained. This gave WP of 3.02 kg/m³ and 3.99 kg/m³ in the entire catchment. In addition, wheat and maize crops were analysed. For WaPOR, the crops WP was estimated from TBP and ETa at the area covered, while for SWAT+, the crops WP were estimated from grain yield and ETa at a few studied hydrological response units levels. WaPOR gave average annual TBP, ETa and WP of 23160.7 kg/ha/year, 779.1 mm/year, and 2.98 kg/m³ respectively for wheat. And, 24018.5 kg/ha/year, 836.2 mm/year, and 2.92 kg/m³ respectively for maize.

With SWAT+, wheat gave average annual ETa values of 560.5 mm/year and 563.1 mm/year at two HRUs studied (HRU 1621 and HRU 1584), and maize gave 833.7 mm/year and 788.1 mm/year (HRU 257 and HRU 1614). Average annual wheat crop yields of 1261.7 kg/ha/year and 1530.0 kg/ha/year, and for maize yield, 5444.5 kg/ha/year and 3159.1 kg/ha/year were obtained. Therefore, wheat crop WP of 0.23 kg/m³ and 0.27 kg/m³, and maize crop WP of 0.65 kg/m³ and 0.40 kg/m³ were obtained. Maize gave higher WP components than wheat in both approaches, but with differing crop WP.

However, results of this study should caution users concerning SWAT+'s current capacity to accurately simulate biomass time series in a catchment. The model does not implement all calculations, and hence, the output generation on crop yields and land cover management is not fully available. Also, the complex nature of the micro climatic conditions of the study area leading to uncertainty in the weather input data, may have highly influenced the results in both WaPOR and SWAT+.

Keywords: WaPOR, SWAT+ model, water productivity, total biomass production, actual evapotranspiration, crop yield.

ACKNOWLEDGEMENTS

First and foremost, I thank God for His sufficient grace for seeing me through this far, and everything that this thesis has turned into. I'm deeply grateful to the Dutch government through NUFFIC scholarship program for this great opportunity.

Sincere thanks to my supervisors: Chris Mannaerts, for the opportunity to undertake this interesting topic, which enabled me to explore my passion, particularly in this field. Your guidance provided very insightful and helpful solutions to the challenges I encountered. Your encouraging remarks gave me a sense of confidence, and kept me going. To Ben Maathuis, your unending support in the WaPOR part of my study is genuinely acknowledged. Thank you for providing me with the tools I required in accomplishing this part of the main tasks, and for your replies to my impromptu emails whenever I needed help. I will always admire your commitment to seeing the best out of your students. To Harm-Jan Benninga, last but not least, of the supervisory crew; I am extremely thankful for your invaluable contribution towards this entire process, and your positive criticism that helped nurture my growth in the scientific research field. Thank you for always creating time to answer my 'lame' questions, making sure I was on the right track. And even when it got tough, you encouraged me to keep moving.

Though words would never be enough for me to express my gratitude, the accomplishment of this thesis is also as a result of individuals' contribution, that wouldn't go unmentioned. Many thanks to Yasser Abbasi (PhD) for always being ready to assist in any possible way in solving my model problems. Thanks for allowing me to knock on your door on short notice, and even after COVID19 kicked in, your help extended in emails, and for that I'm forever grateful. To Megan Blatchford (PhD), thanks for helping in conceptualizing and setting the tone in my research topic during the very early stages. Even though it was just the beginning, this was a big deal for me, and I hope you will be proud of this final product. To Sammy Njuki (PhD), my gratitude to you goes a long way, but mostly, thanks for just being there, and I mean, in all aspects. *Absante kwa kumionyesha njia, Mungu akubariki.*

I am extremely thankful to Chris George and the entire SWAT user groups fraternity, for their tremendous support with the model; to the virtual friends I met and kept in touch afterwards. Special thanks to Pauline from WRMA (and former ITC student) for her endless efforts in getting me the streamflows data. *Ubarikive milele.*

My fieldwork wouldn't have been possible without Joost Hoedjes' help. It was a pleasure interacting with you, and thanks for making it a success. Also, thanks for introducing me to Paul Ruoya who was very kind to facilitate my activities in the field. I extend my gratitude to Edward Muchiri, for his kind help in additional data acquisition, and to my former Professor, John Gathenya, for pulling strings on this one.

I would like to express my gratitude to eleaf for the internship opportunity, which was a whole learning experience for me, both professionally and in personal life. This provided more insight to my forthcoming thesis. Many thanks to the Gatimus for hosting me in Wageningen during this period.

Many thanks to the teaching staff at the ITC Faculty, especially in the WREM department, for their commitment in instilling theoretical as well as practical skills and knowledge on remote sensing and water-related studies. To the staff and administration for ensuring a comfortable study stay, and even when the COVID19 pandemic kicked in. To my advisor, Arno van Lieshout, for his encouragements, frequent check-ups, making sure my classmates and I are all okay and safe. I would like to encourage my juniors, Patience and her classmates, who are still walking the walk, to keep on keeping on. I acknowledge my fellow classmates, friends and my Kenyan community (*wakurugenzi wakuu*) for making this stay feel like home, even though away from home. This has been an awesome experience, we'll do it again, God-willing!

Finally, lots of appreciation to my support system: my relatives in Europe, aunt Nanyama who made this possible for me in more ways than she probably knows, and aunt Hellen, for their moral support and encouragement. To my family and friends back at home, my brothers Wafula and Wandabwa, my sisters Sylvia, Caro, Irene and Kate, and my uncle Alfred, your prayers have kept me going and at last it is finally done. *Hatimaye!*

TABLE OF CONTENTS

1.	Introduction	1
1.1.	Background and relevance	1
1.2.	Research Objectives	3
1.3.	Novelty of the study.....	3
1.4.	Structure of the thesis	4
2.	Literature Review.....	5
2.1.	Concepts of Water Productivity.....	5
3.	Study Area.....	11
3.1.	Location	11
3.2.	Topography	11
3.3.	Hydrology	12
3.4.	Climate.....	12
3.5.	Socio-economic activities	13
4.	Fieldwork Survey	15
4.1.	Evaluating land cover data	15
4.2.	Crop growth information	17
4.3.	Land cover map	17
5.	SWAT+ Model Water Productivity Analysis.....	19
5.1.	Concept of hydrological water balance	19
5.2.	Datasets	20
5.3.	SWAT+ model set up	23
5.4.	Calibration and validation processes on surface runoff	28
5.5.	Average annual water balance analysis	32
5.6.	TBP, ETa and TBWP simulations analysis	32
5.7.	Wheat and maize crop analysis.....	36
6.	WaPOR Water Productivity Analysis.....	39
6.1.	Methodological approach.....	39
6.2.	Results analysis at yearly basis.....	40
6.3.	Results analysis at dekadal timestep.....	47
6.4.	Wheat and maize crop results analysis	48
7.	Conclusion and Recommendation	51
7.1.	Conclusion	51
7.2.	Challenges and limitation	51
7.3.	Recommendations	52

LIST OF FIGURES

Figure 1.1 Flowchart diagram outlining the general research methodology	4
Figure 2.1 Conceptual diagram of the ETLook model	6
Figure 2.2 Schematic representation of the carbon fluxes; Gross Primary Production (GPP), Net Primary Production (NPP), Net Ecosystem Production (NEP) and Net Biome Production (NBP) (FAO, 2019).....	8
Figure 3.1 Location of the Lake Naivasha basin, indicating distribution of studied farm fields and hydro-meteorological stations	11
Figure 3.2 Average monthly rainfall and daily maximum and minimum temperature in a month.	12
Figure 4.1 The Lake Naivasha basin locations surveyed with the specific cover crops	15
Figure 4.2 Harvested wheat with pivot irrigation equipment on site (left) and overgrown wheat after harvesting (right) at Kijabe farm.	16
Figure 4.3 Maize at maturity stage, on a farm at Kinangop area (left) and dry ready to harvest maize on a farm at the upstream part of the catchment (right)	16
Figure 4.4 Cropping seasons for specific crops in years 2019-2020 in Lake Naivasha basin	17
Figure 4.5 Land cover from Sentinel-2 imagery (29/01/2018 and 01/02/2018)	18
Figure 5.1 TAHMO against CHIRPS monthly precipitation at station TA00414 (2018-2019)	21
Figure 5.2 TAHMO against CHIRPS monthly precipitation for station TA00416 (2018-2019)	21
Figure 5.3 Average annual precipitation from CHIRPS plotted against elevation for the 7 stations	22
Figure 5.4 SRTM DEM data for Lake Naivasha basin.....	24
Figure 5.5 Delineated Lake Naivasha basin	25
Figure 5.6 Lake Naivasha basin soil classification map	26
Figure 5.7 Observed and simulated flows at channels 61 plotted against precipitation at monthly timestep	31
Figure 5.8 Observed and simulated flows at channels 10 plotted against precipitation at monthly timestep	31
Figure 5.9 Schematic representation of the average annual water balance components in the catchment	32
Figure 5.10 Simulated ETa [mm] plotted against precipitation at monthly timestep for the entire catchment ...	33
Figure 5.11 Simulated ETa [mm] plotted against precipitation at monthly timestep in period 2009-2012	33
Figure 5.12 Simulated TBP plotted against precipitation at monthly timestep for the entire catchment	34
Figure 5.13 Visual representation of the simulated annual means ETa [mm] and TBP[kg/ha] of the catchment for the period 2009-2019	35
Figure 5.14 Wheat and maize yield from Nyandarua county office against SWAT+ simulations at specific HRUs	36
Figure 6.1 Yearly spatial distribution of WaPOR ETa [mm/year] in Lake Naivasha basin across the study period (2009-2019).	42
Figure 6.2 Yearly spatial distribution of WaPOR TBP [kg/ha] in Lake Naivasha basin across the study period (2009-2019).	44
Figure 6.3 Yearly spatial distribution of WaPOR TBWP [kg/m ³] in Lake Naivasha basin across the study period (2009-2019)	46
Figure 6.4 Time series representation of ETa [mm/dekad] and TBP [kg/ha/dekad] for years 2009-2019	47
Figure 6.5 Time series representation of TBWP [kg/m ³] at dekadal time-step	48

LIST OF TABLES

<i>Table 1.1 Specifications of available WaPOR Version 2.1 datasets in the portal adapted from Mul & Bastiaanssen (2019)</i>	2
<i>Table 5.1 Location of the two TAHMO stations</i>	20
<i>Table 5.2 Location information on the five gauge stations</i>	23
<i>Table 5.3 Meaning description of the soil map classes adopted from Tiruneh (2004).</i>	27
<i>Table 5.4 Soil physical properties required by SWAT+ model</i>	27
<i>Table 5.5 Land use land cover (LULC) classes details</i>	28
<i>Table 5.6 Sensitivity analysis with their ranks on parameters regarding streamflow</i>	30
<i>Table 5.7 Average annual TBP, ETa, and TBWP obtained in the entire catchment</i>	35
<i>Table 5.8 Wheat crop WP simulated results</i>	37
<i>Table 5.9 Maize crop WP simulated results</i>	37
<i>Table 6.1 Provided WaPOR Level II datasets used for Lake Naivasha basin in this study</i>	39
<i>Table 6.2 Yearly statistics of WaPOR ETa [mm/year] (2009-2019) over the catchment.</i>	41
<i>Table 6.3 Yearly statistics of WaPOR TBP [kg/ha/year] (2009-2019) over the catchment.</i>	43
<i>Table 6.4 Yearly statistics of WaPOR TBWP [kg/m3] (2009-2019) over the catchment.</i>	45
<i>Table 6.5 Mean annual wheat ETa, TBP and TBWP across the 2009-2019 period.</i>	49

ACRONYMS AND ABBREVIATIONS

WP	Water Productivity
TBP	Total Biomass Production
ETa	Actual evapotranspiration
TBWP	Total Biomass Water Productivity
SWAT	Soil and Water Assessment Tool
WaPOR	Water Productivity Open-access portal of Remotely-sensed data
GDP	Gross Domestic Product
GEPIC	GIS-based Environmental Policy Integrated Calculator
SWAP	Soil Water Atmosphere and Plant
TAHMO	Trans-African HydroMeteorological Observatory
CHIRPS	Climate hazards group infrared precipitation data
ILWIS	Integrated land and water information system
NCEP CFSR	National Centers for Environmental Predictions, Climate Forecast System Reanalysis
SUF12	Sequential Uncertainty Fitting version 2
SWAT CUP	Soil and Water Tool Calibration and Uncertainty Program
IPEAT+	Integrated Parameter Estimation and uncertainty Analysis Tool Plus
SRTM	Shuttle Radar Topography Mission
VITO	Vision on Technology for a better world
UNESCO-IHE	IHE Delft Institute for Water Education
IWMI	International Water Management Institute
WRMA	Water Resources Management Authority
FAO (UN)	Food and Agriculture Organization of the United Nations

1. INTRODUCTION

1.1. Background and relevance

The physical water scarcity across the globe poses a threat on agricultural productivity, especially with the current rapid population growth in many countries, leaving the countries facing challenges in the water and food sector. FAO (2011) states that the agricultural production will require to increase by 70% by the year 2050 in order to oblige to the foreseen 40% population rise.

In Kenya, agriculture plays a key role in the country's social and economic development as it contributes to about 60% of the total export earnings and accounts for 26% of the country's Gross Domestic Product (GDP) (Adimo, 2016). In provision of sustainable water and food security in Kenya among other semi-arid countries in Africa, policies and actions have been implemented with efforts to boost land and water productivity (Molden, 2007). In Kenya, the Water Act 2002 recognizes water as important natural resources as well as a basic human right (Ministry of Water and Irrigation, 2007). The agricultural policy governs the utilization of these resources to improve agricultural growth by promoting different diversity in crops, as well as environment protection especially the degraded areas and catchments (Alila & Atieno, 2006).

Water productivity (WP) is defined as the biophysical or economic benefits per unit amount of water required or used in provision of these benefits. This is applied on agriculture; crop or livestock, forestry, fisheries and more. In physical WP, the slogan 'more food per drop' is often used referring to the ratio of mass of agricultural output to the amount of water consumed (Molden et al., 2007). Crop water productivity (CWP) [kg/m^3] is defined as the ratio of harvestable crop yield [kg/ha] to the amount of evapotranspiration [m^3/ha] (Zwart & Bastiaanssen, 2004). Crop yield is the marketable product of biomass, evapotranspiration is the actual crop water consumed, which consists of transpiration from plants and evaporation from the soil.

Different scales including plant level, farm field, basin, national and global levels as well as their inter-relationships (depending on user-defined goals), are essential when analysing agricultural WP (Molden, Murray-Rust, Sakthivadivel, & Makin, 2003). For instance, J. Liu et al. (2008) conducted an analysis at global scale (124 countries) using the GEPIC crop model and found that 80% of the countries have potential to improve their water productivity, with the present farm management practices. Also, Zwart & Bastiaanssen (2004) carried out a field survey and found that there was a huge difference in WP among the investigated crops, mainly due to climate variation and farm management practices at that moment.

Different approaches have been applied in studies on quantifying WP. Cai et al. (2009) categorizes these into four approaches: (i) Field experiments, which provide detailed information on WP but are limited to local scale. (ii) Crop-hydrological modeling, which is focused on hydrological processes in relation to plant growth at a catchment extent. For instance the Soil and Water Assessment Tool (SWAT) model adopts this approach. (iii) Coupling of a hydrological model with information from remote sensing as a source for the model input data. (iv) Adopting geo-spatial application tools only, which is advantageous in mapping WP across different spatial as well as temporal scales.

WaPOR (FAO, 2020) was launched by the Food and Agriculture Organization of the United Nations (FAO-UN) on April 20th 2017. The portal provides open access to remotely sensed datasets that enable monitoring

of land and water productivity across Africa and the Near East. The derived data sets cover the period from 01/01/2009 to present at temporal scales that vary from daily to dekadal, seasonal and annual. WaPOR targets stakeholders from local farmers to decision makers with an aim of increasing agricultural production by monitoring WP. The consortium of the WAPOR project include ITC, eleaf, VITO, UNESCO-IHE, IWMI, and WaterWatch Foundation.

The derived remote sensing-based datasets cover different regions at three spatial levels. (i) Level I (250 m resolution) products are available at continental scale over Africa and the Near East. (ii) The level II (100 m resolution) products cover a selected set of countries (21) and river catchments (4) including Jordan River basin, Nile River basin and Niger River basin. (iii) Level III (30 m resolution) covers selected irrigation schemes (8 so far) in Egypt, Mali, Lebanon, Ethiopia, Mozambique, Kenya and Sudan (FAO, 2019). Table 1.1 shows details of the data sets available on the WaPOR portal.

Table 1.1 Specifications of available WaPOR Version 2.1 datasets in the portal adapted from Mul & Bastiaanssen (2019).

Thematic area	Layers	Level I (250 m)	Level II (100 m)	Level III (30 m)
Climate	Precipitation	Daily (5 km)		
	Reference Evapotranspiration	Daily (20 km)		
Water	Actual Evapotranspiration and Interception	Dekadal/annual	Dekadal/seasonal/annual	Dekadal/seasonal/annual
	Evaporation			
	Transpiration			
	Interception			
Land	Total biomass production	Dekadal/annual	Dekadal/annual	Dekadal/annual
	Land cover classification			
	Phenology			
WP	Gross WP	Annual	Seasonal	Seasonal
	Net WP	Annual	Seasonal	Seasonal

With an aim to ensure that WaPOR datasets are efficient to users, quality assessment via validation and comparative analyses have been (and are still ongoing) conducted by researchers on different WP data components. Most of these researches are MSc and PhD theses, and are discussed in Mannaerts et al. (2018) and Mul & Bastiaanssen (2019).

Blatchford et al. (2019) validated Version II of WaPOR ETa against insitu measurements (from 14 eddy covariance (EC) stations) across Africa and obtained an overall estimation of R² and RMSE of 0.6 and 1.04 mm/day respectively. She also found out that there was a consistency in the time series trend at the 3 levels, especially for Level I and II, as influenced by the regions' climatic conditions.

Teshite (2018) compared WaPOR Level III to AquaCrop model WP estimates in Wonji sugarcane plantation, upper Awash basin Ethiopia. Results indicated that WaPOR above ground biomass production (AGBP) estimates were consistently lower than the AquaCrop and in-situ AGBP estimates. Hence a lower WaPOR WP estimates (1.43-3.46 kg/m³) compared to the model estimates (2.49-5.39 kg/m³) were obtained.

He recommended that further studies to be conducted in assessing WaPOR WP components by exploring in-situ measurements as well as the use of other approaches.

1.2. Research Objectives

1.2.1. Main Objective

The main objective of this research is to compare WaPOR remote sensing-based level II WP estimates to SWAT+ model-based WP estimates in Lake Naivasha basin, Kenya.

1.2.2. Specific Objectives

The specific objectives are:

- i. To evaluate the spatial distribution of different land cover types present in Lake Naivasha Basin.
- ii. To simulate SWAT+ model TBP and ETa.
- iii. To analyze WAPOR level II products TBP, ETa and TBWP.

1.2.3. Research Questions

- i. What types of land covers are found in Lake Naivasha Basin? And how are they spatially distributed in the catchment, especially the rainfed and irrigated crops?
- ii. How does SWAT+ simulate its WP components? Which input parameters in the model are sensitive in the calibration and validation process?
- iii. How do WaPOR WP estimates compare to SWAT+ in the catchment?

This research hypothesizes that WAPOR remote sensing-based and SWAT+ model-based WP estimates are comparable.

1.3. Novelty of the study

SWAT+ is a new version of the SWAT model, completely restructured with high flexibility and added capabilities such as a reduced number of database files, which can be utilized depending on user application (Bieger et al., 2017). The SWAT model (Arnold, Kiniry, et al., 2012) is a physical-based, semi-distributed hydrological model that performs simulations on crop growth, hydrological balance (surface and groundwater), water quality, and sediment transportation at defined small to large catchment scale on a daily continuous time steps (Arnold & Fohrer, 2005).

SWAT can also be used for predicting the long term impact of changing climatic conditions, soil characteristics, land cover types, topographic features, and farm practices within a catchment. It operates on a daily time step with up to monthly or annually output time-step. It is widely applied globally, and proved to work efficiently for different regions applications (Arnold & Fohrer, 2005). With its open coding access and technical support from the user groups, the model has the ability to function with tool interfaces for pre- and post-processing, parameterization and calibration. GIS interfaces have been developed for QGIS and ArcGIS.

An advantage of the SWAT model over other crop-hydrological based models such as AquaCrop and SWAP, is that the crop biomass and water consumption estimates in relation to availability of water resources are accounted for (Vaghefi et al., 2017).

Past researches have been conducted using SWAT in modeling the hydrological processes and water quality in Lake Naivasha basin, Kenya. Some of these researches have targeted the lake Naivasha, while others focussed on a particular sub-catchment. For instance, Makau (2018) estimated sediment transportation in

the Malewa sub-catchment. Lukman (2003) analysed the impact of climate change variability on the lake levels. Muthuwatta (2004) focussed on the fluctuation of the lake levels as well on estimating spatial distribution of stream flows in the Gilgil and Malewa sub-catchments. The novel aspect of this research is to establish a SWAT+ model for the Lake Naivasha basin, especially focused on simulating the biomass and ETa which are then compared to WaPOR estimates.

1.4. Structure of the thesis

The structure of this thesis consists of seven chapters. Chapter 1, Introduction gives a brief background and relevance of the research topic, which leads to the objectives, questions, and novel aspect of the research. Chapter 2, Literature review provides an overview of the concepts of WP and the tools to estimate the WP components from both WaPOR and SWAT+. In chapter 3, the study area characteristics including geographical position, climate, topography and hydrology, are described. Chapter 4, Fieldwork survey provides insight to the study area; the land cover and crops data collected. This is in fulfillment to the first specific objective of this research.

Chapter 5 fulfills specific objective (ii) as it discusses the SWAT+ model concepts, required input datasets, procedures and results. Chapter 6 discusses the calculations and results of WaPOR WP components (specific objective (iii)). Chapter 7, Conclusion summarizes SWAT+ WP results in comparison to WaPOR WP results in fulfillment of the main objective. It also provides a reflection on the research process in general, challenges encountered and recommendations for future studies. Figure 1.1 shows general overview of the methodology approach.

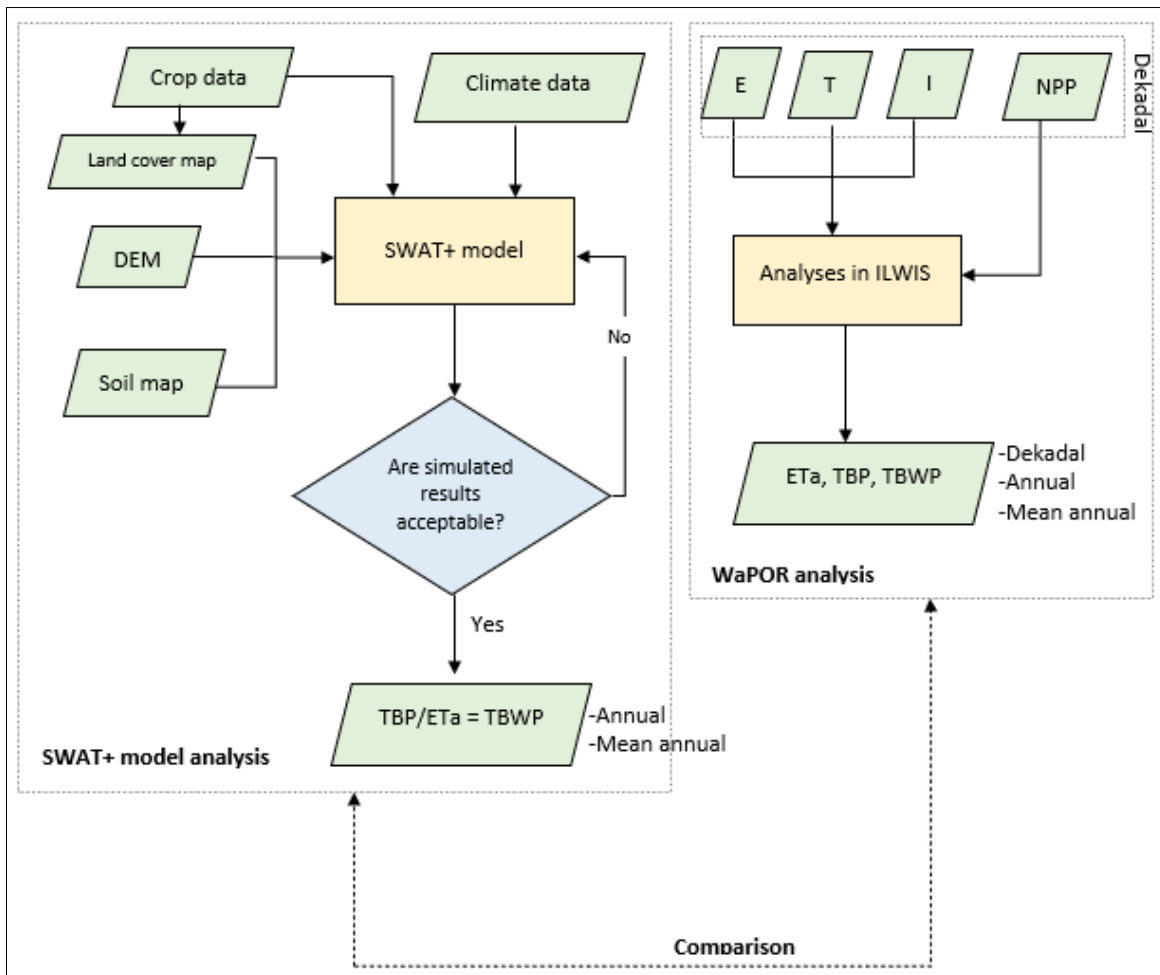


Figure 1.1 Flowchart diagram outlining the general research methodology

2. LITERATURE REVIEW

2.1. Concepts of Water Productivity

In agricultural crop production, WP is derived as a function of biomass output obtained in relation to amount of water input to the plants. The output is measured in terms of accumulated biomass or crop yield, whereas the water input is measured in terms of actual evapotranspiration.

Water productivity components are influenced by factors including: (i) Geographical location of the region of interest, which determines accessibility to resources that facilitate adequate water productivity. (ii) Climatic conditions. Precipitation plays a key role. Other weather factors are air temperature, solar radiation, relative humidity and wind speed, which control the evapotranspiration. (iii) Environmental factors including topographic and soil properties of the region, and the land cover. (iv) Land and water management practices, which include supplementing rainfed agriculture with irrigation systems, nutrients supply, pest and diseases control, among others (Blatchford, 2016).

WaPOR estimates the WP intermediate components basically from satellite datasets. The SWAT+ on the other hand, models hydrological processes and plant growth to estimate both ETa and accumulated biomass from which WP is later calculated externally from the model.

2.1.1. Actual evapotranspiration

Actual evapotranspiration is defined as the sum of the amount of water transpired from plants, evaporated from the soils and intercepted rainfall by canopy. ETa is a significant portion of the water balance in a catchment, especially in an arid and semi-arid regions where the ETa demands are met or exceeded (Teixeira, 2008).

For Lake Naivasha basin, different methodologies have been used in past researches to estimate the ETa. For instance Alemseged (2002) used derived satellite data as input to the Surface Energy Balance (SEBS) model (Su, 2002) for estimating ETa at Kijabe wheat farm. Similarly, Njuki (2016) estimated ETa using the SEBS model and compared the outcomes with EC flux measurements to assess irrigation performance at Delamare farm.

WaPOR provides evaporation (E), transpiration (T) and interception (I) separately, primarily at dekadal timestep, which can then be aggregated to seasonal and annual basis (eLEAF, 2020). The ETLook algorithm (Bastiaanssen et al., 2012; Pelgrum, Jehanzeb, & Cheema, 2010) is applied in estimating the E, T and I. It adopts the Penman-Monteith equation (Monteith, 1965) (Equation 2.1) as a two-source model in calculating E and T expressed in Equation 2.2 and Equation 2.3 and calculates I (Equation 2.4) as a function of plant canopy, leaf area index (LAI), and precipitation (FAO, 2019).

$$\lambda ET = \frac{\Delta(R_n - G) + \rho_a c_p \frac{(e_s - e_a)}{r_a}}{\Delta + \gamma(1 + \frac{r_s}{r_a})} \quad \text{Equation 2.1}$$

Where λ is the latent heat of evaporation [J kg^{-1}], E is evaporation [$\text{kg m}^{-2} \text{s}^{-1}$], T is transpiration [$\text{kg m}^{-2} \text{s}^{-1}$], R_n is the net radiation [W m^{-2}], G is soil heat flux [W m^{-2}], ρ_a is air density [kg m^{-3}], c_p is specific heat of dry air [$\text{J kg}^{-1} \text{K}^{-1}$], e_a is actual vapour pressure of the air [Pa], e_s is saturated vapour pressure [Pa] which is a function of the air temperature. Δ is the slope of the saturation vapour pressure against the temperature curve [Pa K^{-1}]. γ is the psychrometric constant [Pa K^{-1}], r_a is aerodynamic resistance [s m^{-1}], and r_s is bulk surface resistance [s m^{-1}].

$$\lambda E = \frac{\Delta(R_{n,soil} - G) + \rho_a c_p \frac{(e_s - e_a)}{r_{a,soil}}}{\Delta + \gamma(1 + \frac{r_{s,soil}}{r_{a,soil}})} \quad \text{Equation 2.2}$$

$$\lambda T = \frac{\Delta(R_{n,canopy}) + \rho_a c_p \frac{(e_s - e_a)}{r_{a,canopy}}}{\Delta + \gamma(1 + \frac{r_{s,canopy}}{r_{a,canopy}})} \quad \text{Equation 2.3}$$

where λE and λT are evaporation [W/m^2] and transpiration [W/m^2] respectively, $R_{n,soil}$ [W/m^2] and $R_{n,canopy}$ [W/m^2] are the net radiations at soil and canopy respectively. r_{soil} [s/m] and r_{canopy} [s/m] are soil and canopy resistances respectively.

$$I = I_{lai} \left(1 - \frac{1}{1 + \frac{c_{veg} P}{I_{lai}}} \right) \quad \text{Equation 2.4}$$

Where I is the Interception, c_{veg} is vegetation canopy, I_{lai} is the leaf area index [-] derived from NDVI [-], and P is the precipitation [mm].

Figure 2.1 indicates that E and T are computed from the surface and sub-surface soil moisture respectively, and the I is estimated from vegetation canopy (FAO, 2019).

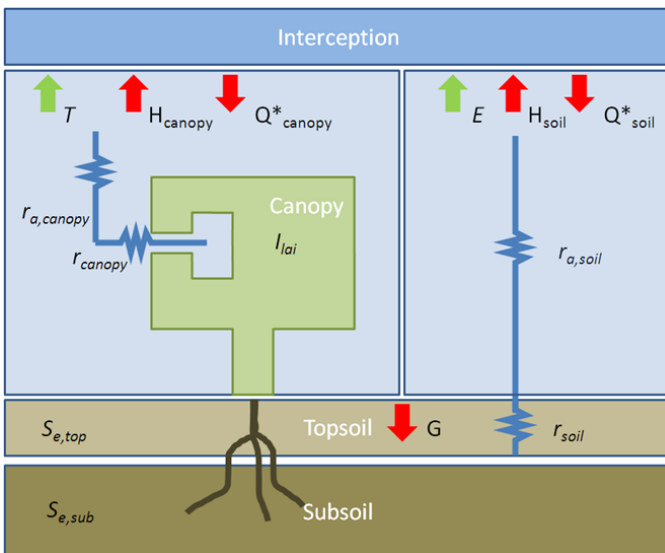


Figure 2.1 Conceptual diagram of the ETLook model

When the three components (E, T, and I) are considered in calculation, Gross WP is obtained as indicated in Equation 2.5. When the plant output is related to only the transpiration, Net WP is obtained (Equation 2.6).

$$Gross\ WP = \frac{Biomass}{E + T + I} \quad \text{Equation 2.5}$$

$$Net\ WP = \frac{Biomass}{T} \quad \text{Equation 2.6}$$

In SWAT model studies, ETa is simulated as a component in the hydrological processes (Equation 5.1) and is represented as a main source of depletion of the fallen precipitation. The ETa is calculated from Potential Evapotranspiration (PET). PET is the amount of water that can evaporate and transpire where there is unlimited water availability. This can be estimated in SWAT+ model via four approaches, namely (i) Priestley-Taylor, (ii) Penman-Monteith, (iii) Hargreaves, or (iv) Read-in external PET values. Similarly to the WaPOR, PET was estimated using the Penman-Monteith approach (Equation 2.1) (Monteith, 1965). Climatic input data including air temperature [°C], solar radiation [MJ/m²], relative humidity [-], and wind speed [m/s] were required in this case (described in section 5.2.1).

The model first calculates the evaporated maximum amount of precipitation that was intercepted by the plant canopy, which varies daily as a function of LAI (Equation 2.7) (Neitsch, Arnold, Kiniry, & Williams, 2005). The amount of intercepted precipitation depends on the land covers. For instance in forests, the amount of evaporated interception can be higher than transpiration. Secondly, SWAT model calculates the maximum soil evaporation and maximum plant transpiration using Ritchie (1972) approach.

$$can_{day} = can_{max} * \frac{LAI}{LAI_{max}} \quad \text{Equation 2.7}$$

where can_{day} is the maximum amount of water that can be withheld in the canopy on a given day [mm], can_{max} is the maximum amount of water that can be withheld when the canopy is fully developed [mm], LAI is the leaf area index for a given day [-], and LAI_{max} is the maximum leaf area index for the plant [-].

Different methodologies have been employed in estimating ETa in a catchment using the SWAT model. Marek et al. (2015) performed calibration and validation of ETa directly against lysimeter insitu measurements. B. Liu & Gan (2018) used derived remote sensing ETa instead of insitu ETa. Tulshiram et al. (2015) obtained ETa estimates after calibrating and validating reservoir storage simulations.

2.1.2. Biomass production

In WaPOR, biomass production is represented as either TBP, AGBP or specific crop yield. TBP is the total accumulated biomass at the end of growing season of a plant. AGBP is obtained by applying a constant conversion factor of 0.65 that represents the ratio of the shoot to the entire plant. Crop yield is the harvestable biomass depending on the specific crop type and is calculated as Equation 2.8 (Mannaerts et al., 2020).

$$Crop\ yield = \frac{HI * \epsilon_{lue}\ cor * \sum_{SOS}^{EOS} NPP}{\alpha * AGBF (1 - \theta)} \quad \text{Equation 2.8}$$

where crop yield is in [ton/ha]. HI is the crop harvest index [-], $\epsilon_{lue}\ cor$ is the plant light use efficiency correction factor [-]. SOS and EOS are the plant start and end of season respectively [day], NPP is the plant net primary production [gC/m²/day], α is the factor that relates NPP to dry matter production (DMP) [tonDM/ha/day], $AGBF$ is the plant above ground fraction [-], and θ is the plant moisture content [-].

The biomass production is obtained as a conversion from the Net Primary Production (NPP) [gC/m²/day] to dry matter production DMP [kgDM/ha/day] using a scaling factor of 0.45 gC/gDM. Therefore 1 NPP [gC/m²/day] is equal to 22.222 DMP [kgDM/ha/day]. The NPP values range between 0 to 5.4 gC/m²/day, that is DMP of 0 to 120 kgDM/ha/day, though higher values of upto 320 kgDM/ha/day can occur (FAO, 2018).

The NPP component is derived from satellite and weather data using the light use efficiency approach (Ruimy et al., 1999) based on Monteith (1972). NPP describes the carbon exchange between the ecosystem and the environment during photosynthesis process (Valentini, 2003) as shown in Figure 2.2.

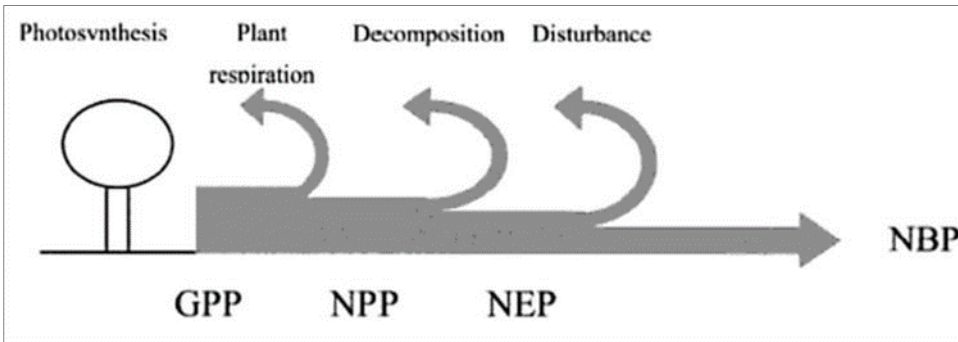


Figure 2.2 Schematic representation of the carbon fluxes; Gross Primary Production (GPP), Net Primary Production (NPP), Net Ecosystem Production (NEP) and Net Biome Production (NBP) (FAO, 2019).

The NPP is computed during a growing season for a particular land cover based on the plant light use efficiency (LUE) in relation to the amount of intercepted photosynthetically active radiation-fraction absorbed by vegetation (f_{APAR}), soil moisture stress, solar radiation, and minimum to maximum temperature ratio. This calculation is based on Monteith (1972) as presented in Equation 2.9.

$$NPP = Sc R_s \epsilon_p f_{APAR} SM \epsilon_{lue} \epsilon_T \epsilon_{CO_2} \epsilon_{AR} [\epsilon_{RES}] \quad \text{Equation 2.9}$$

where NPP is the Net Primary Production, Sc is the scaling factor from DMP to NPP [-], R_s is the total shortwave incoming radiation [G_T/ha/day], ϵ_p is the fraction of PAR (400nm - 700nm) in total shortwave 0.48 [JP/JT], f_{APAR} is the PAR-fraction absorbed (PA) by green vegetation [JPA/JP], SM is the soil moisture stress reduction factor, ϵ_{lue} is the light use efficiency at optimum [kgDM/GJPA], ϵ_T is the normalized temperature effect [-], ϵ_{CO_2} is the normalized CO₂ fertilization effect [-], ϵ_{AR} is the fraction

kept after autotrophic respiration [-], and ϵ_{RES} is the fraction kept after residual effects (including soil moisture stress) [-].

In the SWAT model, plant growth is witnessed from the development of leaf area and canopy height (Allen, Jensen, Wright, & Burman, 1989) influenced by the plant light use efficiency together with weather parameters. Temperature is a significant factor to plant growth, and minimum (base) temperature requires to be attained before a plant development commences. The temperature ranges depend with plant variety. Plant growth process occurs when the accumulated daily temperature exceeds the base temperature until optimum temperature is reached (maturity stage). This is expressed as heat units (Equation 2.10). Heat units is the accumulated heat required by a plant to maturity stage (Neitsch et al., 2005).

$$HU = T_{mean} - T_{base} \quad \text{when } T_{mean} > T_{base} \quad \text{Equation 2.10}$$

where HU is the number of heat units accumulated in a day [-]; where the summation during the growth period gives the total potential heat units (PHU) required for a plant to mature (Equation 2.11). T_{mean} is the mean daily temperature [°C], and T_{base} is the minimum (base) temperature for a plant growth [°C].

$$PHU = \sum_{d=1}^m HU \quad \text{Equation 2.11}$$

where PHU is the total heat units required for plant maturity [-], HU is the number of heat units accumulated on day d , where $d = 1$ on the day of planting, and m is the number of days required for a plant to reach maturity stage.

SWAT+ model utilizes an algorithm that converts heat units to ‘days-to-maturity’ for different species of plants/crops that are defined by the length of growing season (simply the planting date to maturity date). These include seasonal, annual and perennial plants. Plant growth is simulated under adequate water, nutrients and climatic conditions at daily timestep (Arnold et al., 2019).

During photosynthesis process, the model converts the intercepted solar radiation to biomass at a plant specific biomass-energy ratio [[kg/ha]/[MJ/m²]] (Arnold et al., 2019). When the plant reaches maturity stage, it stops uptaking water and nutrients, and transpiration. This gives the accumulated biomass [kg/ha] or crop yield, when the plant is harvested and/or completely removed ‘killed’. Crop yield, the harvestable biomass, is calculated as the product of above ground biomass and harvest index (HI) (Equation 2.12).

$$Crop\ yield = Bioms * HI \quad \text{Equation 2.12}$$

where Crop yield is in [kg/ha]. HI, the harvest index, indicates the amount of above ground biomass contributing to the harvestable portion. It is expressed as a ratio of the weight of dry grains [kg] to the weight of total dry matter [kg] ranging from 0.0 to 1.0 for majority of crops (Sinnathamby, Douglas-Mankin, & Craige, 2017). $Bioms$ [kg/ha] is the above ground biomass on the day of harvest calculated as expressed in Equation 2.13 (Neitsch et al., 2005).

$$Bioms = (1 - fr_{root}) * bio \quad \text{Equation 2.13}$$

where fr_{root} is the fraction of the total biomass in the roots at the day of harvest [-]. bio is the total plant biomass on the day of harvest [kg/ha].

In relation to the specific crop variety, WP can be calculated in terms of the crop yield per unit water use (ETa) as shown in Equation 2.14 (Sadras, Grassini, & Steduto, 2010).

$$CWP = \frac{Crop\ yield}{ETa} \quad \text{Equation 2.14}$$

where CWP is the crop water productivity [kg/m³], crop yield is in [kg/ha], and ETa is the actual evapotranspiration [m³/ha].

The SWAT model has the capability of simulating phenological information as well as growth dynamics of about 80 varieties of crops via the parameters defined. The model also factors in management practices such as tillage operations, and crop residue management in organic matter decay and mineralization processes by soil bacteria and micro-organisms (Arnold et al., 2012). In comparison to SWAT, SWAT+ model has added capability features: two or more crops planted in rotation or growing at the same time can be modeled. Land management practices, such as planting and harvesting dates, can also be modeled by specific user-defined criteria (Bieger et al., 2017).

3. STUDY AREA

3.1. Location

Lake Naivasha basin is located in the Rift Valley in Kenya at latitude 0.15°S to 0.92°S and longitude 36.15°E to 36.40°E (zone 37°S UTM) (Figure 3.1). It is shared between Nyandarua county in the north and west, Nakuru county in the south-east and Narok county in the south-west. Nyandarua county consist of Kinangop, Kipipiri, Ol Kalou, Oljororok and Ndaragua sub-counties.

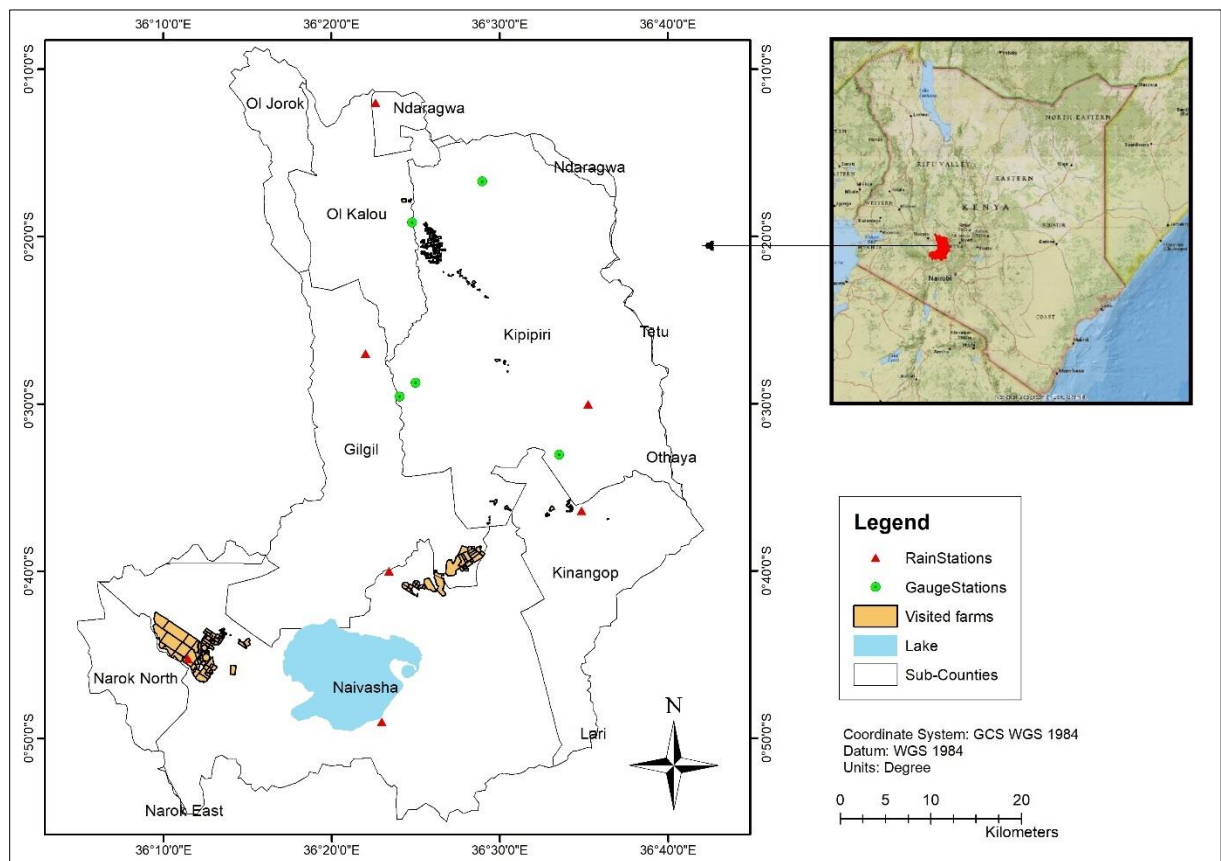


Figure 3.1 Location of the Lake Naivasha basin, indicating distribution of studied farm fields and hydro-meteorological stations

3.2. Topography

Elevation ranges from 1980 m above sea level (masl) at the floor of the Rift Valley near the lake to 3990 masl at the Aberdare Ranges and Mau Escarpments on the eastern and south-west sides of the catchment respectively. High elevations are also witnessed at the far south where Mount Longonot borders the catchment.

3.3. Hydrology

The catchment covers an area of approximately 3400 km² with Lake Naivasha, the 2nd largest freshwater lake in Kenya after Lake Victoria, covering approximately 170km². The lake has no surface outflow, and is famously known as a Ramsar wetland site since 1995 (Becht, Odada, & Higgins, 2005).

Two major perennial rivers from the north are River Malewa which contributes about 80% and River Gilgil which contributes 10% inflow into the lake (Armstrong, 2002). Surface water does not reach the lake on the east, west and south sides during the whole year, because of seasonality of the rivers. River Karati on the eastern side reaches the lake during heavy rains, while others such as River Marmonet from Mau Escarpment recharges at Ndabibi Plains at the western side of the lake. These seasonal rivers contribute about 10% inflow to the lake (Clarke, Woodhall, Allen, & Darling, 1990).

3.4. Climate

The catchment is located in an equatorial tropical region. The climate conditions of the catchment are diverse due to the altitudinal difference, where the upper parts of the catchment experience a humid climate while the lower parts, especially near the lake, experience semi-arid conditions (Becht & Harper, 2002).

The micro climate is experienced with a mean annual rain of about 600 mm at the floor of the Rift Valley and 1500 mm at the Aberdare Ranges (Al-Sabbagh, 2001). This occurs in two rainy seasons; long rains in March to May and short rains in October to November. These are preceded with relatively dry seasons in December to February and June to September respectively. The daily mean maximum and minimum temperatures ranges between 24.6 °C to 28.3 °C and 6.8 °C to 8.0 °C respectively (De Jong, 2011). Figure 3.2 shows the catchment rainfall, maximum and minimum temperature sourced from CHIRPS and NCEP CFSR respectively.

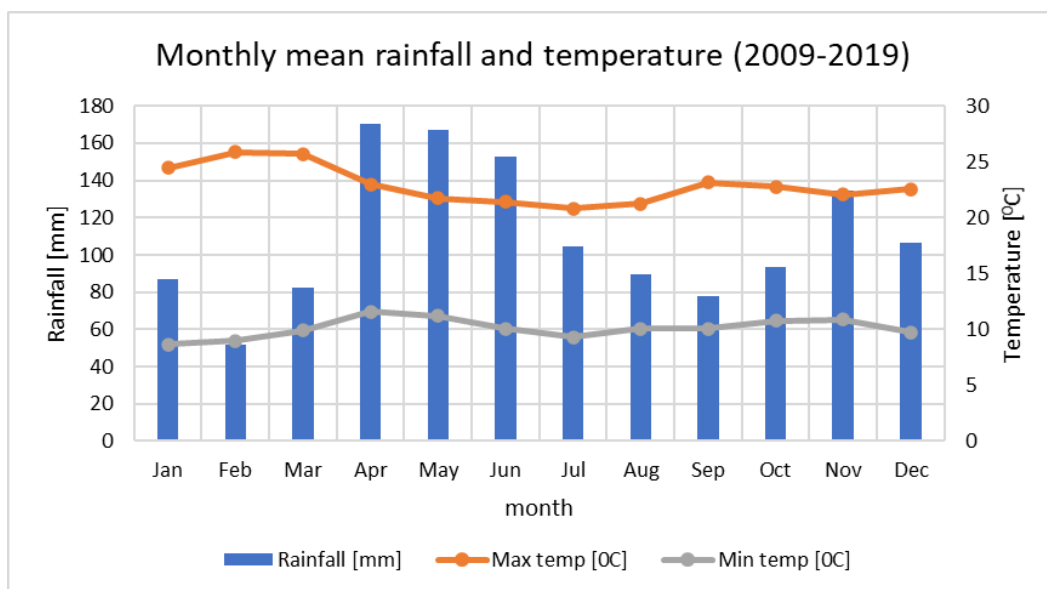


Figure 3.2 Average monthly rainfall and daily maximum and minimum temperature in a month.

3.5. Socio-economic activities

A major portion of the catchment is used for both rainfed and irrigated; subsistence and commercial agriculture purposes. It supports a wide variety of socio-economic activities. The upstream part holds mainly small-scaled farming with cultivated crops such as cereals, vegetables and tuber crops. The downstream part consists of large horticultural and floricultural greenhouses, geothermal projects, fish farming, and inhabited diverse species of wildlife that acts as a tourist attraction. Other parts of the catchment are covered with natural vegetation: forests, shrubs, grassland, and water bodies including the Lake Naivasha and rivers (Odongo, 2016).

4. FIELDWORK SURVEY

Fieldwork was conducted from 8th to 25th January 2020 at different parts of the catchment, targeting both upstream and downstream sections. Locations of ITC weather stations were also used as reference to the targetted farm fields. The main purpose of this fieldwork was (i) To conduct ground-truthing on land cover information in Lake Naivasha basin. (ii) To collect crop phenological information and basic land and water management practices from farmers in the catchment.

4.1. Evaluating land cover data

The ‘*Windshield survey*’ sampling strategy (Defourny, Jarvis, & Blaes, 2014) was employed to target parcels of 0.25 ha or larger sizes that are easily accessed along the roads. The land cover information was collected using ‘*SW maps-GIS and Data Collector*’ mobile application installed on an android phone (SOFTWEL Pvt, 2020). This included both cropland (cereals, tuber crops, vegetables, leguminous, grasses and fodder crops) and non-cropland (shrubland, forests, greenhouses, waterbodies, bare land) covers.

Google Earth Pro (Google Earth, n.d.) was used for counter-checking the land covers and map locations. Photographs together with written notes were also included in the process. Figure 4.1 shows the specific farm fields in Lake Naivasha basin that were surveyed and where land cover crop information was collected.

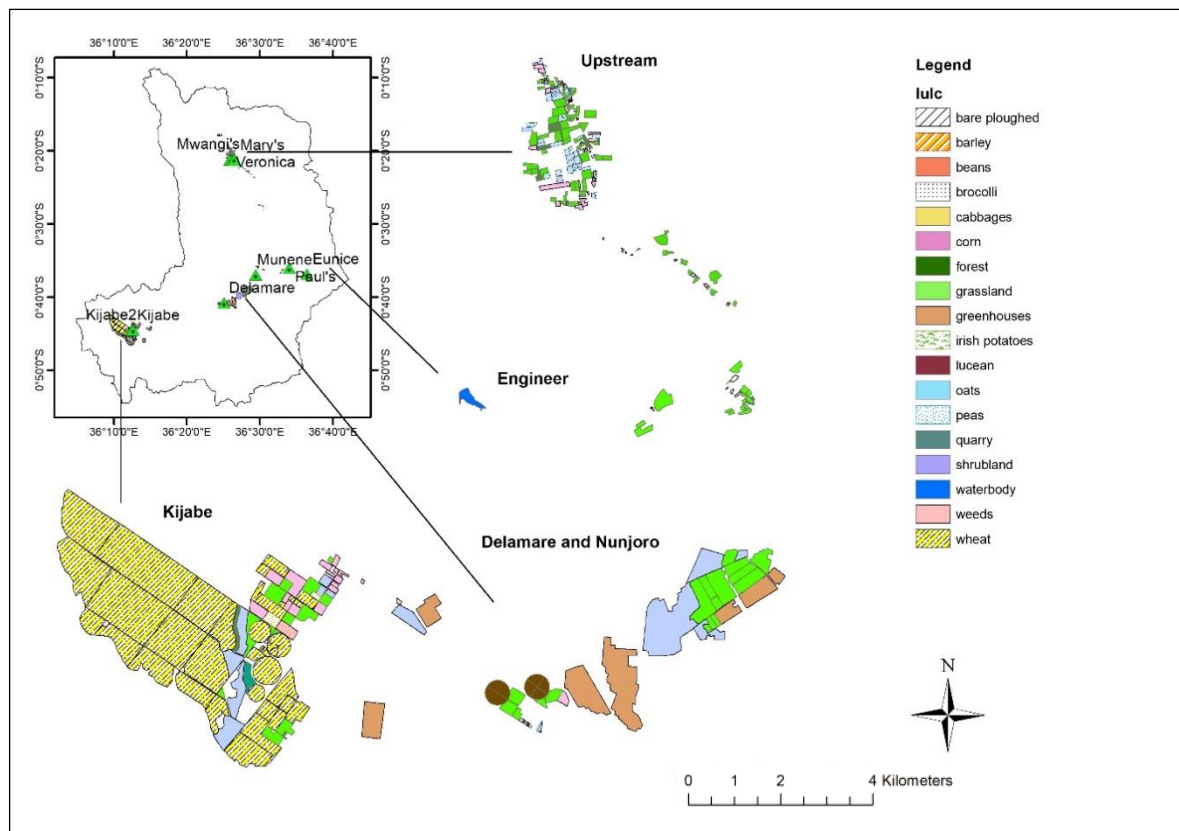


Figure 4.1 The Lake Naivasha basin locations surveyed with the specific cover crops

It was evident that the majority of the farm fields are small, mostly on flat terrain, hence have a large heterogeneity in the land cover. For instance, Kinangop ‘Engineer’ and upstream areas consist of rainfed small scale farmlands with mainly cereal crops and grasslands vegetation. However, it was noticed that some large-scaled farms dominate parts of the catchment downstream. For instance, Kijabe farm at the west of Lake Naivasha mainly consists of large scale wheat growing. Delamare and Nunjoro at the north-eastern side of the lake consist of mainly irrigation schemes growing fodder crops. Figure 4.2 and Figure 4.3 illustrate some of the farm fields visited.



Figure 4.2 Harvested wheat with pivot irrigation equipment on site (left) and overgrown wheat after harvesting (right) at Kijabe farm.



Figure 4.3 Maize at maturity stage, on a farm at Kinangop area (left) and dry ready to harvest maize on a farm at the upstream part of the catchment (right)

The climate in Kinangop area is different from the rest parts of the catchment with lower temperatures that result in frost due to nearby slopes of Aberdare ranges. The frost formation help in weed and pests control. Oats and tuber crops such as irish potatoes are therefore favorable crops in this condition. Other crops also evaluated in this region include grassland, maize, barley, cabbages, and garden peas. These crops are mainly rainfed on which farmers use human labour in planting, weeding and harvesting and some machinery in ploughing.

COMPARISON OF WAPOR RS-BASED TO SWAT+ MODEL WATER PRODUCTIVITY IN LAKE NAIVASHA BASIN, KENYA

In the upstream region, rainfed; grassland, maize and some oats are the main cover crops. Compared to Kinangop area, where the maize was almost at maturity stage, in this region maize was dry and ready for harvest (Figure 4.3). Farmers interviewed, also reported that the delayed harvest was due to the delayed rains in the year 2019. Farmland sizes in this visited region were larger than those at Kinangop area. The climate here was also noticed to be drier than Kinangop.

4.2. Crop growth information

Crop growth as well as land and water management practices information from farmers was collected through interviews and questionnaire sheets (sample shown in Appendix A). Crop information from a total of 5 crop types were obtained from farmers in Lake Naivasha basin. Figure 4.4 shows the calendars obtained for the specific crops.

Crop type	Crop	Feb	Mar	Apr	May	Jun	Jul	Aug	Sep	Oct	Nov	Dec	Jan	
Cereals	Baby corn													
	Normal corn													
	Wheat													
	Barley													
	Oats													
Leguminous crops	French beans													
	Garden peas													
Root-tuber crop	Irish potatoes													
Vegetables	Cabbages													
	Broccoli													
Fodder	Lucerne													

Legend:

Planting phase	Growing phase	Harvesting phase
----------------	---------------	------------------

Figure 4.4 Cropping seasons for specific crops in years 2019-2020 in Lake Naivasha basin

Furthermore, long-term crop information, covering the years 2009 to 2019, was obtained from Nyandarua County Crop Development Department office. This included annual crop yields (that is later discussed in Chapter 5), crop phenological information, farm management practices, and monetary and weight value production data.

4.3. Land cover map

A land cover map created from Sentinel-2 imagery (29/01/2018 and 01/02/2018) was obtained from Njuki (ongoing PhD research at ITC). During the field survey, the ground-truth information collected at the specific field sites, showed that some covers such as, shrubland at the upstream parts of the catchment, reflected on the land cover map. The map seems to have missed the greenhouses in some areas north of the lake, as they might have been recently constructed. Irrigated farms around the lake including Delamare were well represented. It was also noted that, most of the cereals crop lands were captured as grassland and bare land.

The confirmed specific land covers from the field survey were then ‘burnt-in’ in the map. This was basically carried out in a simple stepwise manner using polygon-to-raster conversion, combine, and reclassify tool

operations in ArcGIS. Maize, wheat, oats and alfalfa (Lucerne) were defined as separate classes as they were dominant compared to the other crops on the sites visited. Figure 4.5 shows the land cover map obtained.

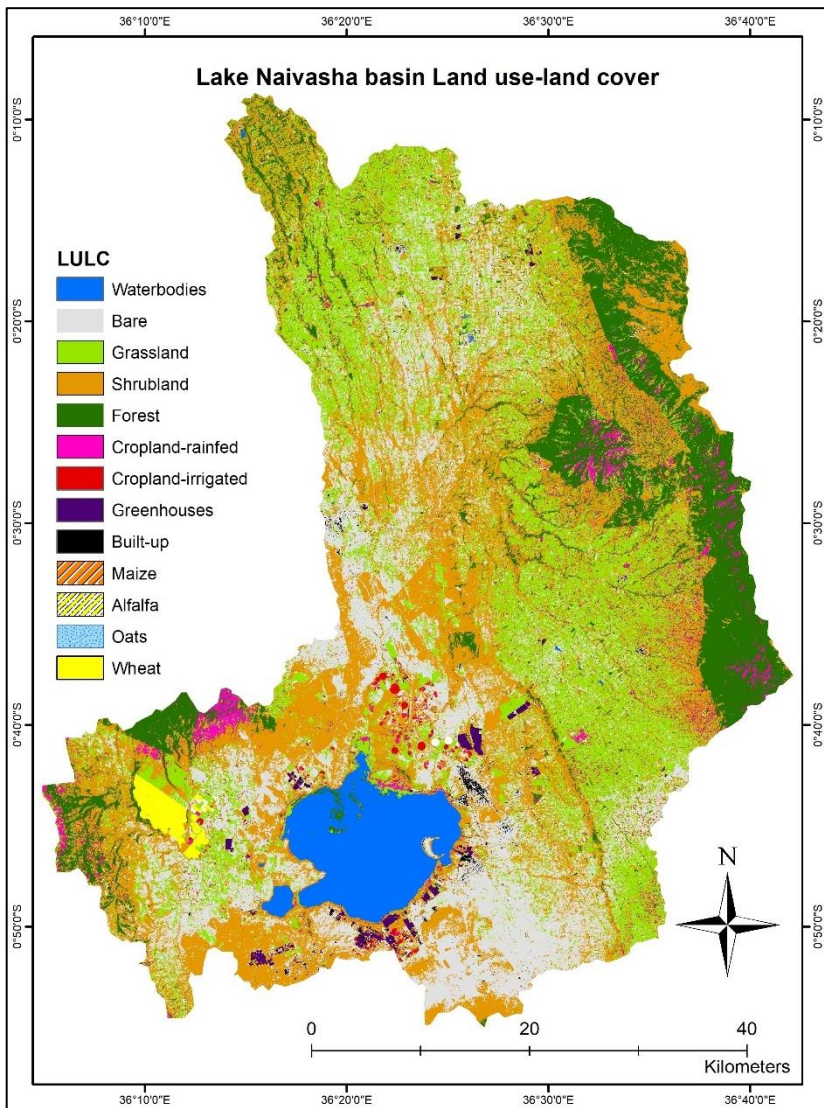


Figure 4.5 Land cover from Sentinel-2 imagery (29/01/2018 and 01/02/2018)

5. SWAT+ MODEL WATER PRODUCTIVITY ANALYSIS

This research adopts the SWAT+ model in building a model for Lake Naivasha basin and simulation of ETa and TBP in the period 2009 to 2019. In comparison to the SWAT model, SWAT+ has improved capability in spatial representation of hydrological processes to achieve the realism in a user-defined catchment.. This is with regard to the catchment delineation and relationships between the spatial objects (sub-basins, hydrological response units (HRUs), channels, inlets and outlets). Users can also define output files at different temporal resolutions (daily, monthly, yearly and average annual), and spatial resolutions (HRU, and basin scale extent) (Bieger et al., 2017). This novel model is, however still improving to fulfil user needs in different application regions with regard to geographical, topographical and climatic characteristics. Bugs and errors in the program are still present and must be fixed.

5.1. Concept of hydrological water balance

In the SWAT+ model, hydrological processes in a catchment takes place in two phases. (i) The land phase, where the amount of water, nutrients and pollutants in a sub-basin are estimated. This occur via infiltration, percolation, evaporation and transpiration processes as well as horizontal exchanges to a channel. (ii) The routing phase, where the actual movement of the water, nutrients and pollutants in a network of channels to the main outlet of the catchment are simulated (Neitsch et al., 2005).

Major hydrological processes in the land phase are quantified based the general water balance equation (Equation 5.1) to comprehend the key water balance components in a catchment. One source of potential uncertainty in the water balance equation is that not all inflows, outflows and storages are fully accounted for (Arnold, Moriasi, et al., 2012).

$$SW_t = SW_o + \sum_{i=1}^t (Preci - SURQ - ETa - Wseep - GWQ) \quad \text{Equation 5.1}$$

where SW_t is the final soil water content after timestep t of day i [mm]. SW_o is the initial soil water content on day t , t is the time [days], $Preci$ is the amount of precipitation on day i [mm]. $SURQ$ is the amount of surface runoff on day i [mm]. ETa is the amount of evapotranspiration on day i [mm]. $Wseep$ is the amount of water seeping into the unsaturated zone from the soil profile on day i [mm]. And GWQ is the amount of return flow on day i [mm].

Precipitation, which is a driving force in hydrological processes, is partitioned into several elements. The falling precipitation may be intercepted by plants or fall on the soil surface, which will either evaporate into the atmosphere, infiltrate or flow as runoff to the main channel. The infiltrated water in the soil may either be taken up by plants, percolate into the aquifer or move laterally to the main channel.

SWAT+ model provides two approaches for estimating surface runoff and infiltration flow. These are (i) the SCS Curve number method (Mockus, 1972) and (ii) the Green & Ampt infiltration method (Green & Ampt, 1912). The SCS Curve number method which is based on daily precipitation and curve number values, was adopted for this research, because it factors in the canopy interception processes, as the plant canopy has a significant influence on the surface runoff as well as ETa and infiltration. On the contrary,

interception is calculated separately when the Green & Ampt infiltration method is used. In estimating the runoff through the stream network, SWAT+ provides two approaches. (i) Variable storage method (Williams, 1969). (ii) Muskingum method (McCarthy, 1938). The default variable storage method was adopted for this research.

5.2. Datasets

The quality of SWAT output greatly depends on the accuracy of the input data. Various past researches conducted on the Lake Naivasha basin have resulted in the availability of a fair amount of data in the ITC archives. However, the quality of this data was questionable, outdated and with gaps. The apparent missing or outdated data needed to be accounted for by updating. Therefore, more sets of data were collected and compared to the already acquired data. In the process, some differences between the data sets were found, and some decisions were made before the data was implemented. This is further explained in the specific sub-sections.

5.2.1. Climate data

With the model approaches for surface runoff, evapotranspiration and plant growth, five weather parameters, namely precipitation [mm], maximum and minimum temperature [°C], solar radiation [MJ/m²], relative humidity [-] and wind speed [m/s] are required. Other parameters are wind direction and atmospheric deposition that were absolutely not required with the chosen model set-up. These parameters are in point data form at the represented meteorological stations, and must be either provided as observed input data or simulated using SWAT+'s weather generator.

It was noted that for the entire period, the ITC and TAHMO measured weather data were unreliable. Inconsistency in the ITC stations data (2017-2019) was due to major gaps that might have resulted from poor maintenance of the rain gauges in the field. On the other hand, most of the TAHMO measured data were unavailable covering only some months in 2018 and 2019. Therefore, the Climate Hazards Group InfraRed Precipitation with Stations (CHIRPS), and the National Centers for Environmental Prediction - Climate Forecast System Reanalysis (NCEP CFSR) weather data for the other variables, were sourced.

5.2.1.1. Comparison of CHIRPS to available TAHMO monthly precipitation

Before CHIRPS precipitation data was adopted as input to the model, a comparison to available TAHMO data (covering March 2018 – Dec 2019 with missing data within) at two measuring stations was conducted to check on reliability of the CHIRPS data in the study region. Table 5.1 shows location information for the two TAHMO rain gauge stations and the comparison results are shown in Figure 5.1 and Figure 5.2.

Table 5.1 Location of the two TAHMO stations

Station	Latitude [°S]	Longitude [°E]	Elevation [m]
TA00414	-0.5866	36.4931	2432
TA00416	-0.6068	36.5811	2488

COMPARISON OF WAPOR RS-BASED TO SWAT+ MODEL WATER PRODUCTIVITY IN LAKE NAIVASHA BASIN, KENYA

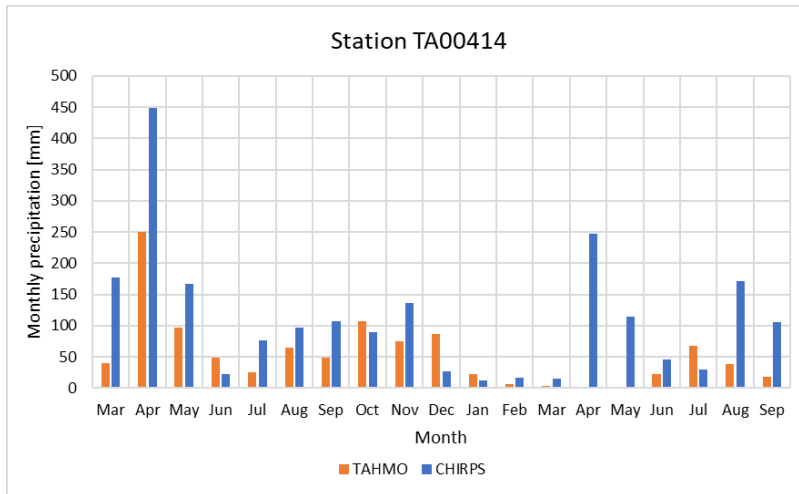


Figure 5.1 TAHMO against CHIRPS monthly precipitation at station TA00414 (2018-2019)

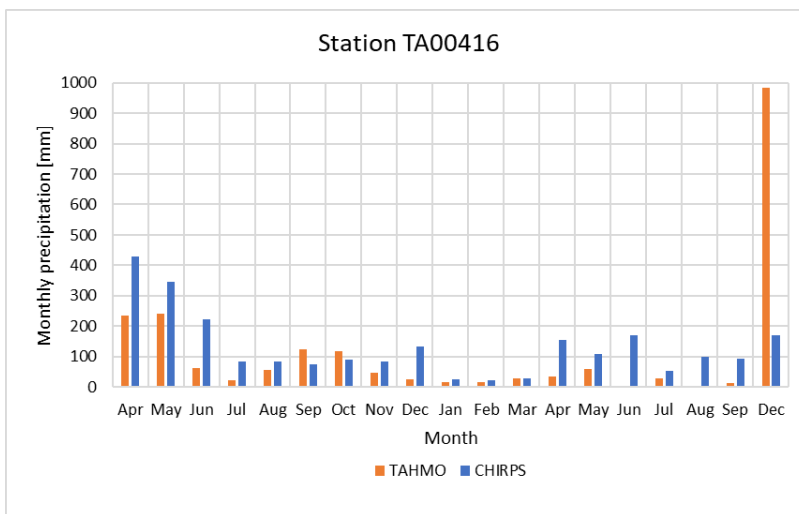


Figure 5.2 TAHMO against CHIRPS monthly precipitation for station TA00416 (2018-2019)

From Figure 5.1 and Figure 5.2, it is evident that CHIRPS precipitation differs from TAHMO at both stations TA00414 and TA00416. However, the trends match the catchment's seasonal pattern of high precipitations in the long rains season (around March-May) and low precipitations in the short rains season (around September-November). It was also evident that January-March of 2019 is a dry period with almost 0 mm precipitation recorded in both stations, as well as by CHIRPS.

Although CHIRPS appears to record higher precipitation than TAHMO in most of the assessed months at both stations, there are a few months where TAHMO recorded equal or higher precipitation especially at station TA00416. In December 2019 even a very high precipitation of almost 1000 mm was reported. This record is probably erroneous when compared to that recorded at TA00414. Therefore, these short-term comparison results were not really able to determine the reliability of CHIRPS data in this study.

5.2.1.2. Weather generator data

Despite having multiple stations in a sub-basin, SWAT+ model utilizes the weather station closest to the centroid of a sub-basin for representing the entire sub-basin weather data. This technique could lead to picking a station with less reliable data. Hence, ‘artificial’ weather stations on the centroids are generated using inverse distance interpolation of the available ‘real’ weather stations, to minimize potential uncertainties (Neitsch, Arnold, Kiniry, & Williams, 2009). Cho et al. (2009) compared the centroid method to precipitation input based on the Thiessen polygons method, and found that the centroid method resulted in higher inaccuracies in simulated data when there is a high spatial variation in the measured precipitation amounts. However, the centroid method is the approach still used in the SWAT+ model.

The weather generator tool generates weather stations data when there is insufficiency in the daily records. This constraint is common in long term data records with ‘missing data’ in the measured records. Also in situations where the weather data is completely unavailable due to lack of operational weather stations. The daily weather values are generated from average monthly data values in each sub-basin with disregard to the spatial variation (Richardson & Nicks, 1990). This weather generator is widely used in SWAT model studies and it is evidenced in a study conducted by Zhang et al. (2004) that in general, the tool is statistically comparable for precipitation, solar radiation, maximum and minimum temperature values when validated against observed data.

5.2.1.3. CHIRPS precipitation data

CHIRPS (Funk, 2018) was adopted to solve the problem of unreliable measured precipitation data from the ITC and TAHMO stations. CHIRPS sources time series (1981 to present) precipitation dataset in raster format at 5 km² spatial resolution. It consist of satellite observed precipitation blended with rain gauge stations data (Dinku et al., 2018).

CHIRPS data for the simulation period (2008-2019) was downloaded from Gorelick et al. (2017) at 7 stations (Figure 3.1) distributed within the Lake Naivasha basin. At each station point, a pixel precipitation value was extracted. To ensure that the values were not erroneous, an average value for the 10 nearby pixels was applied. Figure 5.3 shows the CHIRPS average annual precipitation plotted against elevation at the 7 stations. This shows a positive relationship between the annual precipitation values extracted and the elevation points.

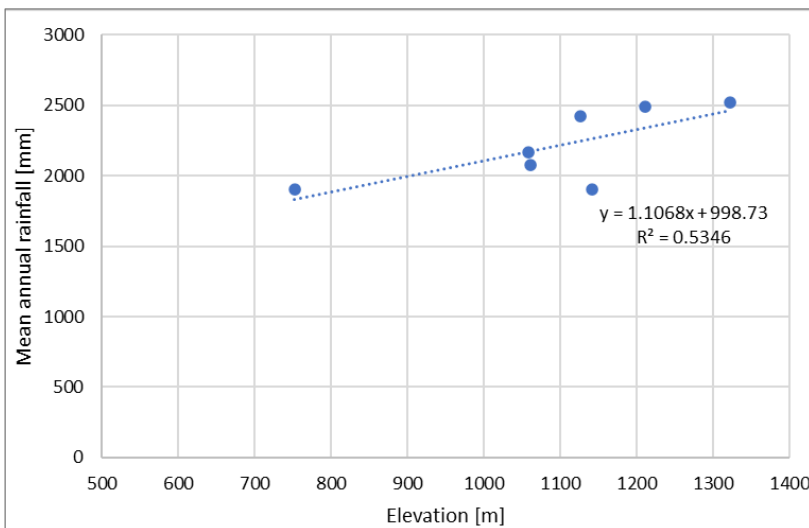


Figure 5.3 Average annual precipitation from CHIRPS plotted against elevation for the 7 stations

5.2.1.4. NCEP CFSR weather data

The US National Centers for Environmental Prediction - Climate Forecast System Reanalysis (NCEP CFSR) data consist of 36 years (1979-2014) of historical weather variables at 38 km² spatial resolution (Saha et al., 2010). NCEP CFSR was sourced for the other weather parameters, namely; maximum and minimum temperature, solar radiation, relative humidity and wind speed. These variables (2009-2014) were downloaded from Texas Agriculture and Management University (2020). And the weather generator was adopted for the remaining 2015 to 2019 period.

5.2.2. Streamflow data

Streamflow data at five gauge stations in Lake Naivasha basin, shown in Figure 3.1 and detailed in Table 5.2 were acquired from the ITC archive. This data was found to be incomplete and outdated regarding the years 2007-2014 (Abbasi, Mannaerts, & Makau, 2019). Hence, an updated set of streamflow data at the five stations was acquired from WRMA Naivasha. This data values still differed much from the ITC data, apart from at gauge station 2GB04 and 2GB05. This could be probably due to different quality control methods used from both parties. These include handling and or imputation of missing data, and checking and removal of outliers.

Table 5.2 Location information on the five gauge stations

Station	X-Coordinate [m]	Y-Coordinate [m]	Elevation [m]
2GB04	219808.8	9969175.2	2334
2GB05	210688.5	9945446.0	1987
2GB08	212081.6	9964640.5	2264
2GC04	212451.6	9946983.4	2000
2GC05	228295.2	9939060.7	2408

The streamflow data was measured by reading water levels [m] at daily basis from a gauging staff and then converted to flow rate [m³/s] using rating curves developed by Meins (2013). It was recommended by Makau (2018) and Ochieng (2017) that an update on the rating curves should be conducted by including recent acquired streamflow data sets. This would help improve future analysis of simulated compared to the observed streamflows.

5.2.3. Crop Yield data

Actual sampled annual crop yields from farmers in Nyandarua county were obtained from the County Crop Development Department office. This included different cereals, tuber crops, leguminous, pyrethrum, vegetables and fruits. Only maize and wheat yields were used for this research. The sampled crop yields cover the study period but with missing data for 2013. These yields data were used for the validation of simulated crop yields at specific hydrological response units (HRUs).

5.3. SWAT+ model set up

In this research, SWAT+ modeling was conducted in SWAT+ Editor version 1.3.0 and QSWAT+ version 1.3.3 in QGIS version 3.4.11. These software are open source and QSWAT+ is equipped with capability of visualization of simulated results graphically and dynamically over time, which is advantageous compared to other SWAT platforms like ArcSWAT (Y. T. Dile et. al., 2016). Basically, the following steps were implemented: (i) Watershed delineation, (ii) Creating HRUs, (iii) Writing input files, and (iv) Running the model.

5.3.1. Watershed delineation

Following the step-by-step procedure guidelines in the QSWAT+ user manual (Y. Dile, Srinivasan, & George, 2015), the SWAT+ model for Lake Naivasha basin was created. Topography information from SRTM Digital Elevation Model (30 m resolution) (Figure 5.4) was acquired from USGS (2018). The Lake Naivasha basin is identified as an endorheic catchment (that is catchment with only an internal outlet) where the river network converge into the lake. A sink 'hole' (less than 1000m) was therefore, created in the lake to identify the lowest elevation point. This is due to the difficulties of the Terrain Analysis Using Digital Elevation Models (TauDEM) (Tarboton, 2015) river network and catchment delineation software used by SWAT model. The model still recognized the southern part of the catchment as lowest point during the delineation process. This issue however did not affect this research, as the focus was on biomass and ETa outputs. The DEM was then projected to a projection coordinate system (WGS 84 UTM zone 37°S) to fit the SWAT+ model requirement.

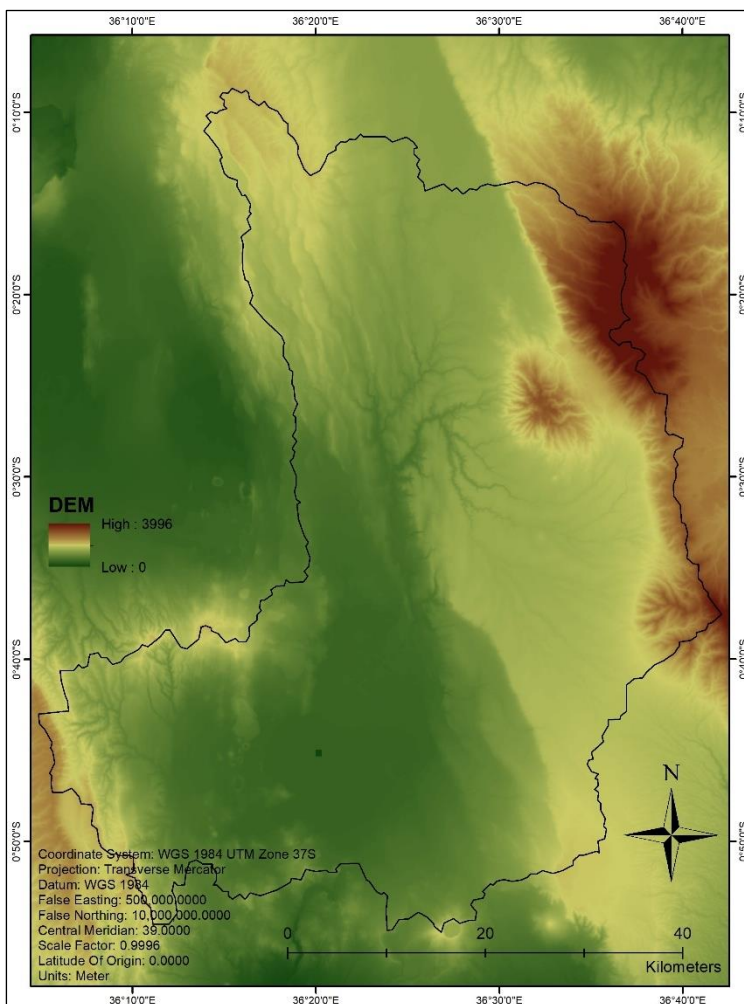


Figure 5.4 SRTM DEM data for Lake Naivasha basin

The lake and a main outlet at the most downstream point of the catchment were then defined generating 15 sub-basins as shown in Figure 5.5.

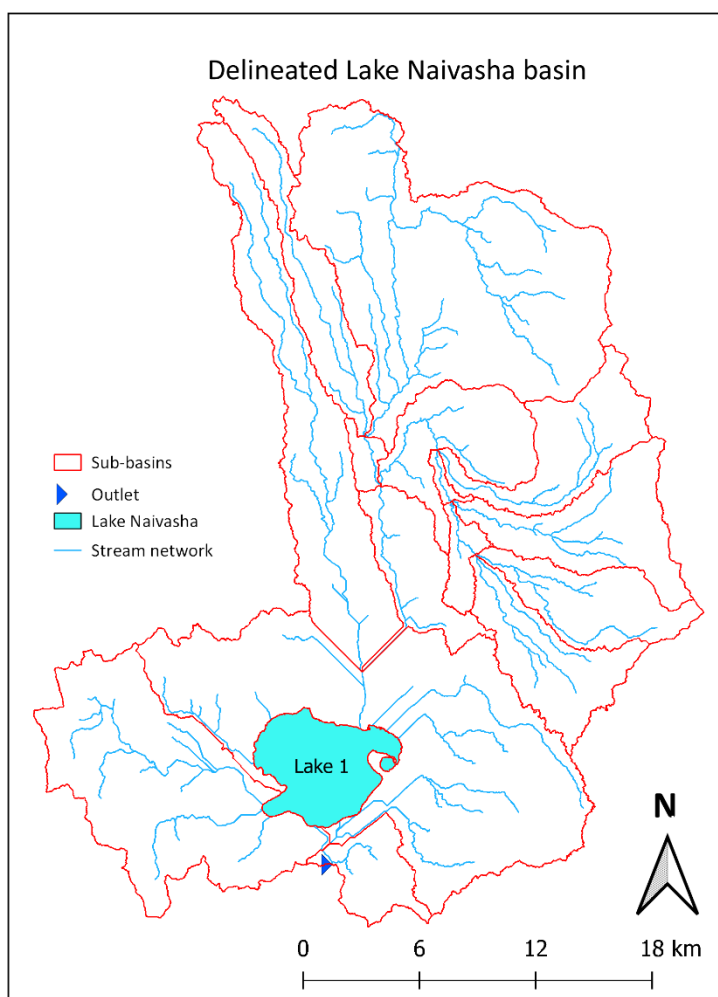


Figure 5.5 Delineated Lake Naivasha basin

5.3.2. Creating Hydrological response units (HRUs)

The delineated sub-basins were further subdivided into HRUs, which are the smallest units within the model. They consist of homogeneous areas of uniform land cover, soil type, and slope range with disregard to the spatial aspect. At each HRU, streamflow is simulated separately and then routed to the sub-basin. HRUs enhance the accuracy in crop heterogeneity hence hydrological processes simulation in a catchment (Arnold, Kiniry, et al., 2012).

The number of HRUs is limited by considering the percentage thresholds in land cover, soil and slope to decrease the run time of the model. These thresholds have a minor effect on streamflow, but a major effect on nutrients simulations with a high sensitivity to soil types and slope (Her, Frankenberger, Chaubey, & Srinivasan, 2015). Thresholds of 20%, 10%, and 20% on land cover, soil and slope respectively were applied, which are the default setting in SWAT (Winchell, Srinivasan, Di Luzio, & Arnold, 2010). An exemption from the thresholds was made to irrigated cropland, alfalfa, corn and oats land covers as they covered smaller areas. 15 sub-basins with 187 channels and 1832 HRUs were generated, covering 96.31% (327155.04 ha) of the total delineated catchment area. The Lake Naivasha covers the remaining 3.69% (12080 ha).

5.3.2.1. Soils definitions

Lake Naivasha basin is of a volcanic type of soils and majorly consist of clay silt texture. Figure 5.6 shows the soil classification map that was developed by the Kenya Soil Survey (Macharia, 2004), acquired from the ITC and ISRIC SOTER (2010) databases. It consist of 23 soil classes, for which physical and chemical properties details are provided in Sombroek, Braun, & van der Pouw (1982). This was then projected to same projected coordinate system as the DEM (WGS 84 UTM zone 37°S).

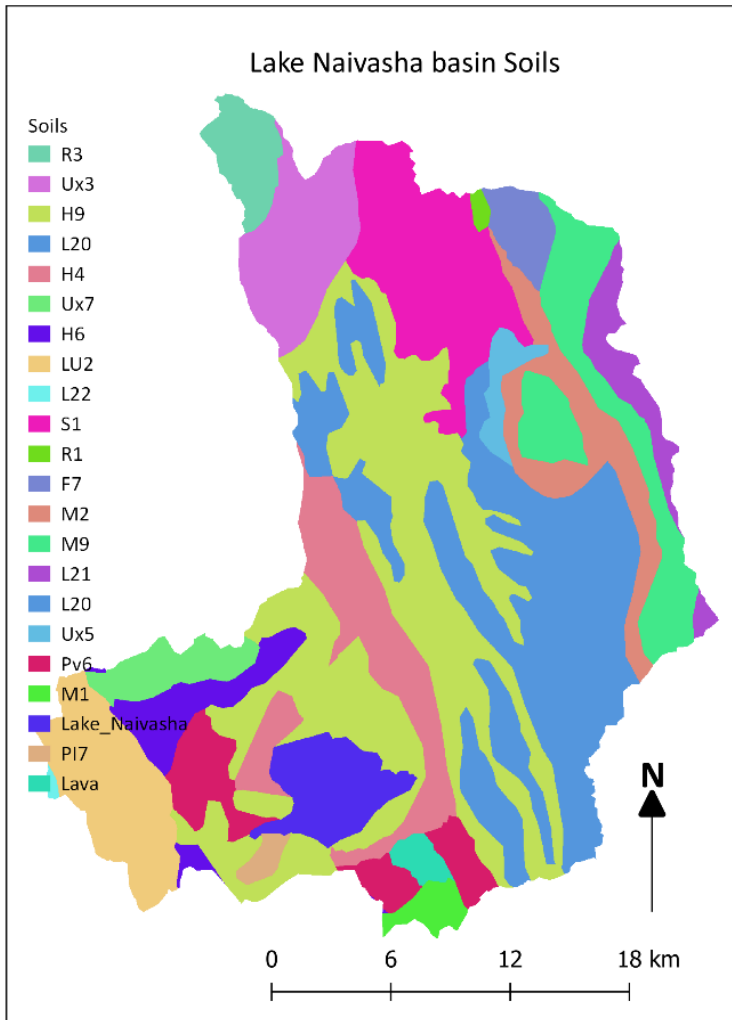


Figure 5.6 Lake Naivasha basin soil classification map

Table 5.3 gives the soils type description of the soil classes as shown in Figure 5.6. Becht et al. (2005) found out that soils in the catchment are very permeable with a low water holding capacity especially around the lake. Parameterization of the soil map was adopted still from Tiruneh (2004) after his fieldwork expedition. This included physical properties as explained in Table 5.4. These were then translated to the SWAT+ model as user lookup tables in csv file format.

COMPARISON OF WAPOR RS-BASED TO SWAT+ MODEL WATER PRODUCTIVITY IN LAKE NAIVASHA
BASIN, KENYA

Table 5.3 Meaning description of the soil map classes adopted from Tiruneh (2004).

Soil name	Description
R3	Well drained
Ux3	Deep to very deep, silty clay (brown clay)
H9	Shallow-well drained, very bouldery or stony loam to clay loam
L20	Well drained, moderately deep to very deep clay, loam to clay
Pi11	Well drained, moderately deep to deep, fine gravelly, sandy-clay loam to sandy clay, with humic top soil
H4	Rocky and stony, clay loam, rock out crops
Ux7	Well drained shallow, dark brown stony loam, with a stone surface dissected older piedmont plain
H6	Deep to very deep, clay loam with a thick humic top soil
LU2	Well drained, deep to very deep, clay loam with a thick humic topsoil
L22	Well drained, deep to very deep clay loam, imperfectly drained, deep cracking clay
R1	Well drained, extremely smeary clay with an acid humic topsoil
F7	Well drained, deep to very deep friable clay with an acid humic topsoil
M2	Well drained, very deep clay loam to clay
M9	Imperfectly drained, shallow to moderately deep loam to clay loam rock out crops
L21	Imperfectly drained, deep very dark firm clay, silty clay loam of thick top soil
Ux5	Well drained, very deep friable and slightly smeary clay with a humic topsoil
Pv6	Excessively drained to well-drained, very deep, loose fine sand to very fine sandy loam (silt)
M1	Excessively drained, shallow to moderately deep stony to gravelly clay loam
PI7	Imperfectly drained to poorly drained, very deep silt loam to clay with a humic topsoil

Table 5.4 Soil physical properties required by SWAT+ model

Soil parameter	Description
NLAYERS	Number of soil layers in soil (1 to 10) [-]
HYDGRP	Soil Hydrological group (A, B, C, D) [-]
SOL_ZMX	Maximum rooting depth [mm]
ANION_EXCL	Fraction of porosity from which anions are excluded [-]
SOL_CRK	Potential or maximum crack volume (optional) [-]
TEXTURE	Texture of soil layer (optional) [-]
SOL_Z	Depth from soil surface to bottom layer [mm]
SOL_BD	Moist bulk density [g/cm ³]
SOL_AWC	Available water capacity of the soil layer [-]
SOL_K	Saturated hydraulic conductivity [mm/hour]
SOL_CBN	Organic carbon content [%]
CLAY	Clay content [%]
SILT	Silt content [%]
SAND	Sand content [%]
ROCK	Rock fragment content [%]
SOL_ALB	Moist soil albedo [-]

5.3.2.2. Land use definition

The land cover determines the amount of intercepted precipitation as well as the impact of the rain drops that hit the soil for instance contributing to nutrients transportation and soil erosion. The obtained land cover map (Section 4.3) was projected to same projected coordinate system as the DEM (WGS 84 UTM zone 37°S). The respective classes were then defined according to SWAT model classes using a look-up table in csv format. Details of the defined land cover classes are provided in Table 5.5.

Table 5.5 Land use land cover (LULC) classes details

Class value	Original LULC	Swat code	SWAT LULC meaning	Watershed area [%]
1	waterbodies	WATR	Water	1.03
2	bare	SWRN	South western range + bare	19.70
3	grassland	PAST	Pasture/hay	26.17
4	shrubland	RNGE	Range shrubland	31.01
5	forest	FRST	Mixed forest	14.24
6	cropland-rainfed	AGRR	Row crops	2.15
7	cropland-irrigated	AGRL	Generic crops	0.53
8	greenhouses	UCOM	Urban commercial	0.56
9	built-up	URML	Urban medium density	0.17
10	maize	CORN	Maize (120 days)	0.08
11	alfalfa	ALFA	Alfalfa (perennial)	0.03
12	oats	OATS	Oats (150 days)	0.02
13	wheat	SWHT	Spring wheat (150 days)	0.62

5.3.2.3. Slope definition

In addition to land cover and soil properties, the slope variation in a catchment dictates the flow direction and speed of water. Spatial distribution of the soil classes in the catchment indicated that 55.79% of the catchment falls within 0-10 % slope range, 20.54% of the catchment lies in 10-20 % slope range and the remaining 19.98 % catchment have a slope of >20 %.

5.3.3. Writing input and output files

After the catchment delineation and generation of HRUs, the prepared daily weather data and model parameter settings (Arnold, Kiniry, et al., 2012) were written as inputs to the SWAT+ Editor (Tech, 2019). The model simulation was then run first for 11 years (2009-2019) with a 2 years warm-up period (2007-2008). The warm-up period enables the model to adopt realistic initial conditions based on the input data before providing results. The model outputs are in *.txt file format, which can be exported back to QGIS for visualization (graphs, maps or animation time series) via QSWAT+.

5.4. Calibration and validation processes on surface runoff

A calibration process is conducted by adjusting the model inputs including parameters with an aim of minimizing differences between observed and simulated data. Afterwards, validation is conducted to evaluate the reliability of the adjusted parameters on an independent set of data. Calibration and validation processes are, therefore conducted at distinct time periods and perhaps also spatiality on hydrological, management-based or plant related simulations.

Generally, both automatic and manual techniques are implemented in the calibration and validation of SWAT model simulations studies. Several automatic algorithms, which were developed for SWAT, have been updated so as to be compatible with the new SWAT+ model. These include IPEAT JAMES+ (Yen et al., 2019), SWATplus-CUP (Abbaspour, 2015), and SWATPlusR (Schuerz, 2019).

Two of the three mentioned algorithms were adopted but were unsuccessful due to several challenges. IPEAT JAMES+ Version 1.0.0 was reported to be still under development. SWATplus-CUP Version 1.0, using the Sequential Uncertainty Fitting (SUFI-2) algorithm, (one month license) with the limitation of calibrating only monthly streamflow simulations, resulted in unresolved challenges that required it to be updated due to the current often updated SWAT+ released versions.

Manual calibration and validation was opted for with parameters within their defined ranges at a monthly timestep. Simulations at monthly timestep are reported to perform better than simulations at daily timestep (Moriasi et al., 2007). However, the attempt to manually calibrate and validate the streamflow dataset was unsuccessful, and resulted to unresolved errors. SWAT+ model developers reported that this is mainly because the model is very new and still has several components under development.

In addition, Arnold et al. (2012) explains that challenges that may arise during calibration and validation process include the availability of sufficient observed data, calibration adjustments distorting the real physical representation of a catchment system by the model, predicting conditions beyond the model capability, among others. In the end, no calibration was, therefore, applied in this study. However, parameter values of the well calibrated SWAT2018 model by Abbasi et al. (2019) on the Malewa sub-catchment, which covers approximately 55% of the Lake Naivasha basin, were used. A sensitivity analysis was performed and the uncalibrated streamflow results at gauges 2GB04 and 2GB05 were analyzed.

5.4.1. Sensitivity Analysis

A sensitivity analysis is performed to analyze the effect of changing model parameters on the output results. Since SWAT in general consists of a huge number of parameters that could be calibrated, identified parameters from previous researches on Lake Naivasha basin were used to identify the key parameters.

The two types of sensitivity analysis are (i) local; where parameter values are changed at one-at-a-time (OAT) basis, and (ii) global; where multiple parameter values are allowed to change simultaneously. Global methods take into account that the sensitivity of one parameter depends on other parameters, but a large number of simulations is required. OAT on the other hand is limited to the fact that, correct values of other parameters, which are fixed during the sensitivity analysis, are never known (Arnold, Moriasi, et al., 2012). In this study, OAT as the default method in SWAT+ model was used.

OAT sensitivity analysis was first conducted by adjusting parameters from their baseline values and assessing the overall streamflow percentage change over the study period. A total of 16 parameters (Table 5.6) regarding streamflow (same as (Abbasi et al., 2019)) were evaluated, but only 7 parameters were found to be sensitive.

Table 5.6 Sensitivity analysis with their ranks on parameters regarding streamflow

Rank	Parameter	Description	Absolute limits	Variation [%]	Q % change
1	SOL_K	Hydraulic conductivity of the soil [mm/h]	0 – 200	±30	±0.39
2	SOL_Z	Depth of the soil layer [mm]	0 – 2000	±30	±0.24
5	CN2	SCS runoff curve number per land [-]	35 – 95	±30	±0.15
3	ESCO	Soil evaporation compensation coefficient [-]	0 – 1	±30	±0.12
4	PERCO	Deep aquifer percolation fraction [-]	0 – 1	±30	±0.10
6	TRNSCH	Transmission losses from channel to deep aquifer fraction [-]	0 – 1	±30	±0.03
7	SOL_AWC	Available water capacity in the soil [-]	0.01 – 1	±30	±0.01
8	ALFA	Baseflow alfa factor [day]	0.15 – 0.50	±30	±0.00
8	GW_DELAY	Groundwater delay [day]	0 – 500	±30	±0.00
8	FLO_MIN	Threshold depth outflow from shallow aquifer [mm]	1 – 500	±30	±0.00
8	REVAP_MIN	Threshold depth of water in the shallow aquifer [mm]	0 – 1000	±30	±0.00
8	REVAP_CO	Groundwater “revap” coefficient [-]	0.02 – 0.4	±30	±0.00
8	OVN	Manning’s value for overland flow [-]	0.01 – 30	±30	±0.00
8	N	Manning’s value for the main channel [-]	0.01 – 0.5	±30	±0.00
8	K_CH	Main channel hydraulic conductivity [mm/h]	0.01 – 173	±30	±0.00
8	SURLAG	Surface runoff lag coefficient [-]	0 – 4	±30	±0.00

The streamflow simulations are highly sensitive to parameters that control the amount of water in the soil layers. These include SOL_K, SOL_Z and SOL_AWC. ESCO directly affects the evaporation from soil. CN2 determines the amount of water that infiltrates from soil surface, and that is converted to runoff. TRNSCH and PERCO (known as RCHRG_DP in SWAT model) dictate the amount of water that seeps to deep aquifer. These results could be used in future calibration studies as starting point for streamflow simulation.

5.4.2. Simulated streamflow results

The model uncalibrated simulations on streamflow at channels 10 (gauge 2GB04) and 61 (gauge 2GB05), upstream and downstream in River Malewa respectively, were presented in hydrological graphs (Figure 5.7 and Figure 5.8). At both channels, the simulated streamflow peaks and troughs match the high and low precipitation trend respectively. Gauge station 2GB04 (Figure 5.8) shows large gaps in observed streamflows, while gauge station 2GB05 (Figure 5.7) shows a gap only in years 2015-2016.

COMPARISON OF WAPOR RS-BASED TO SWAT+ MODEL WATER PRODUCTIVITY IN LAKE NAIVASHA BASIN, KENYA

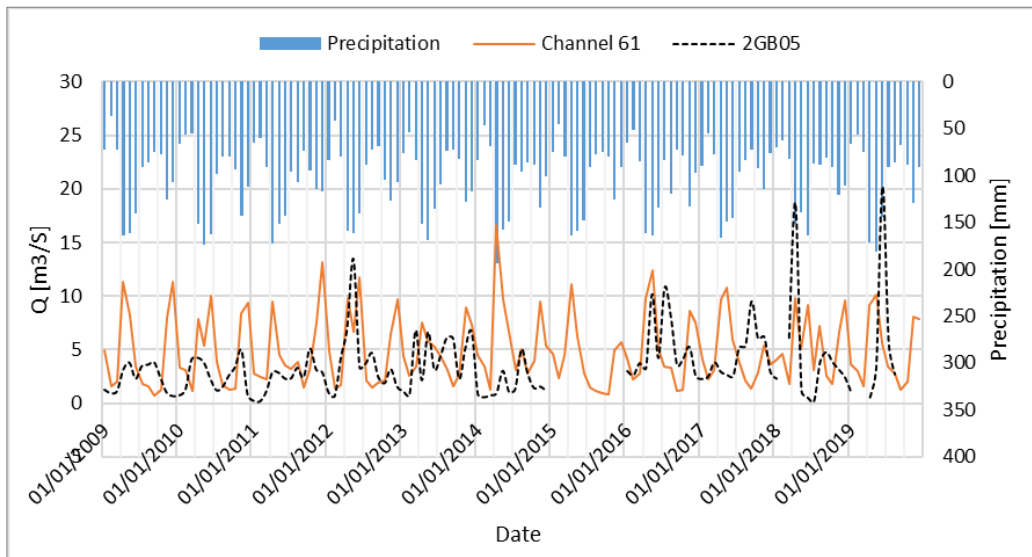


Figure 5.7 Observed and simulated flows at channels 61 plotted against precipitation at monthly timestep

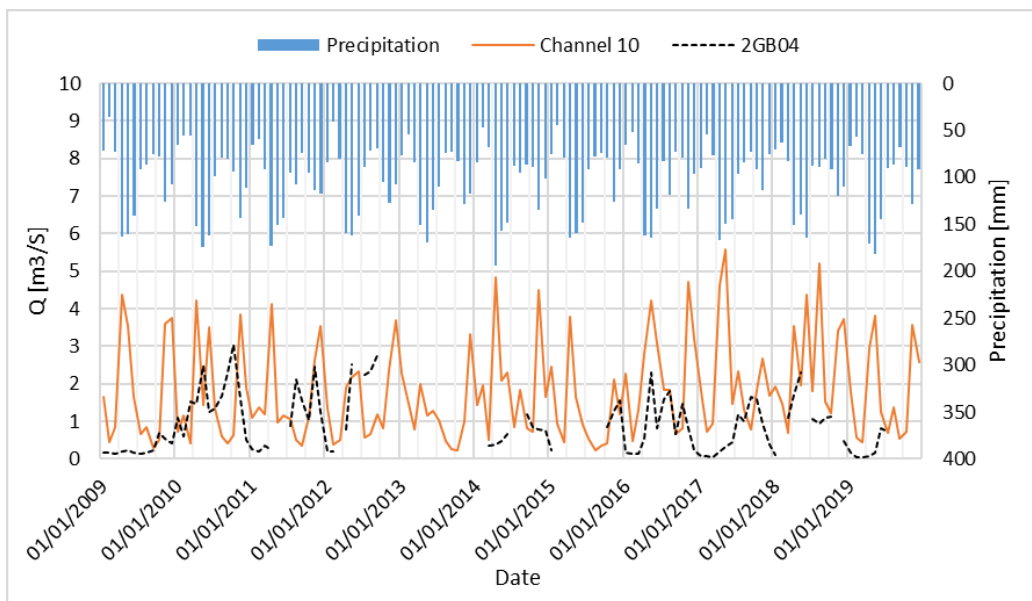


Figure 5.8 Observed and simulated flows at channels 10 plotted against precipitation at monthly timestep

From Abbasi et al. (2019) results, where he adopted SWAT-CUP using SUFI-2 algorithm to automatically calibrate and validate streamflow at the five gauge stations (Table 5.2), he obtained the following results for gauge station 2GB05 and 2GB04: R^2 of 0.86, NSE of 0.64 and PBIAS of 12.93 % (period 2007-2012), and validation results of R^2 of 0.62, NSE of 0.61 and PBIAS of 12.24 % (period 2013-2017) at gauge 2GB05. His validation results at 2GB04 (2016-2017) gave R^2 of 0.84, NSE of 0.80 and PBIAS of 10.05 %.

5.5. Average annual water balance analysis

Despite the model being uncalibrated, the water balance components results were fair when compared to past studies, as good initial parameter settings were applied where possible. An average annual ETa ratio (actual evapotranspiration divided by precipitation) of 0.64, a streamflow ratio of 0.24 and a percolation ratio 0.12 were obtained (Figure 5.9). Abbasi et al. (2019) obtained 0.68 ETa, 0.29 streamflow and 0.13 percolation ratios on the Malewa sub-catchment. Muthuwatta (2004) obtained a streamflow ratio of 0.13 on the Gilgil sub-catchment.

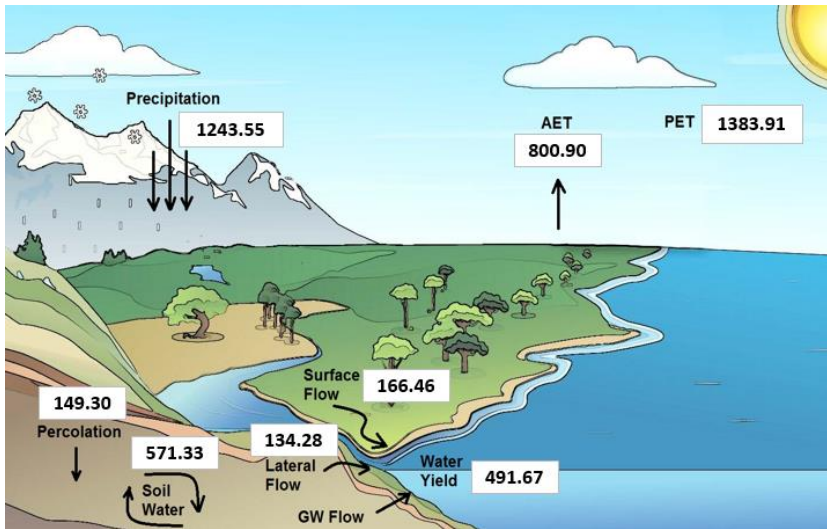


Figure 5.9 Schematic representation of the average annual water balance components in the catchment

5.6. TBP, ETa and TBWP simulations analysis

The ultimate results obtained from the model were ETa [mm] and TBP [kg/ha] (referred to as biomass in the model) at daily, monthly, annual and average annual time step across the simulated 11 years (2009-2019). The simulated products present a limitation in temporal variation over the period frame as CHIRPS precipitation, NCEP CFSR and the weather generator were applied.

The ETa monthly (Figure 5.10), capture the catchment's seasonality with relation to precipitation. The ETa peaks and troughs coincide with the precipitation troughs and peaks respectively. This shows the inverse relationship between ETa and precipitation. The ETa peaks are recorded in the dry season, while the troughs are recorded in the wet season of every year. Figure 5.11 gives a closer look at these results. The ETa peaks tend to fluctuate across the time frame, but the low troughs give a clear pattern of approximately 50 mm in around April and October.

COMPARISON OF WAPOR RS-BASED TO SWAT+ MODEL WATER PRODUCTIVITY IN LAKE NAIVASHA BASIN, KENYA

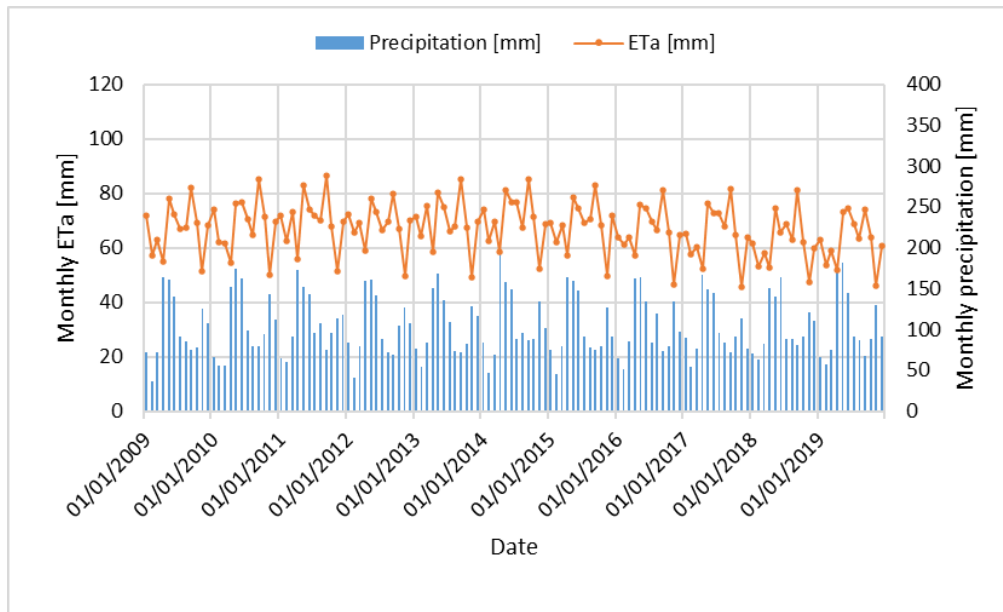


Figure 5.10 Simulated ETa [mm] plotted against precipitation at monthly timestep for the entire catchment

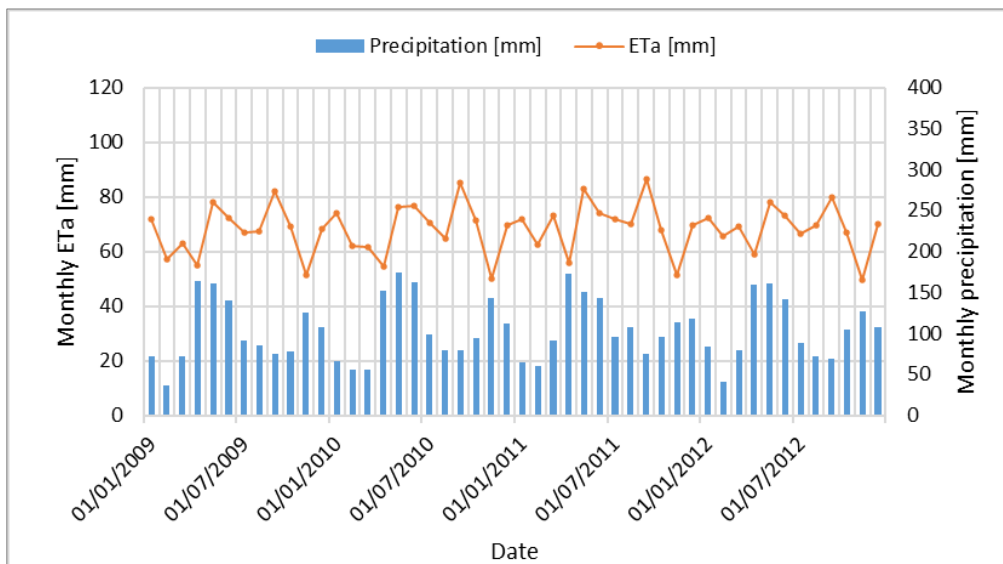


Figure 5.11 Simulated ETa [mm] plotted against precipitation at monthly timestep in period 2009-2012

Figure 5.12 indicate the monthly TBP with a small variation in the values. This is explained by the fact that the model presents the TBP simulations at yearly timestep as shown in Appendix B. The results however show that the TBP peaks match the precipitation high peaks around March to May.

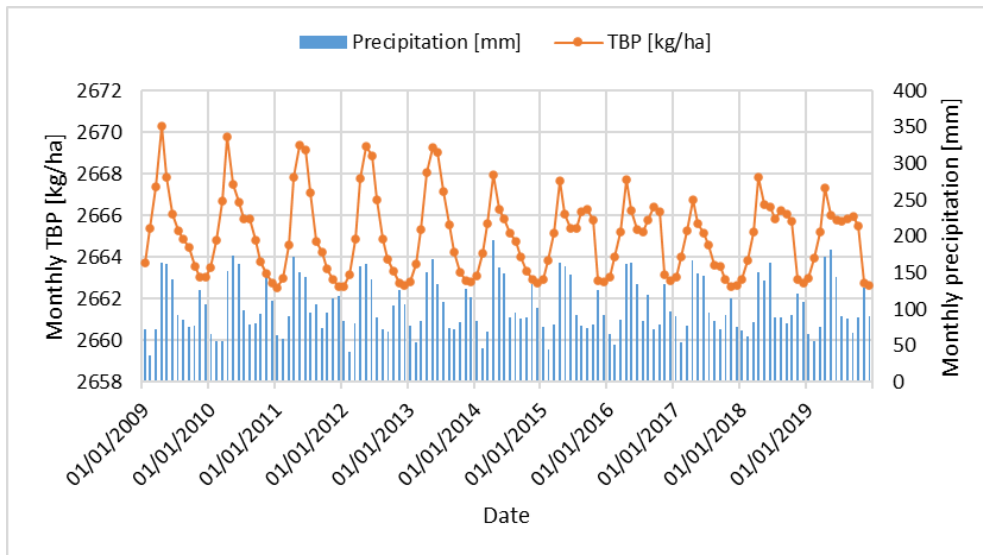


Figure 5.12 Simulated TBP plotted against precipitation at monthly timestep for the entire catchment

Figure 5.13 shows the spatial variation of the average annual ETa and TBP in the catchment. High TBP was recorded at the wetland areas around lake Naivasha, as well as at high altitude (forested) areas at the Aberdare ranges and Mau Escarpment in the north-west and south-east, respectively, of the catchment. Low TBP is indicated at farm lands, for instance at Kijabe wheat farm. This could be due to the seasonal or annual crops that are removed from the farm through harvest and kill at the end of their growing periods.

ETa on the other hand, shows high values at grasslands and at the Kijabe wheat farm. The high ETa at grassland could be due to the less vegetation density thus greater exposure of the soil to evaporation rates. Low ETa estimated are distributed at different areas of the catchment. The high altitude (forested) areas at the Aberdare ranges and Mau Escarpment show moderately high ETa. The soil types as described in Table 5.3 also influence resulted ETa value rates. For example at the northern part of the catchment (upper Gilgil sub-catchment) shows low ETa. This area consist of soil type R3, a well-drained soil, hence less water is left on the surface for evaporation or lower surface flow generation, which is evident from Muthuwatta (2004).

COMPARISON OF WAPOR RS-BASED TO SWAT+ MODEL WATER PRODUCTIVITY IN LAKE NAIVASHA BASIN, KENYA

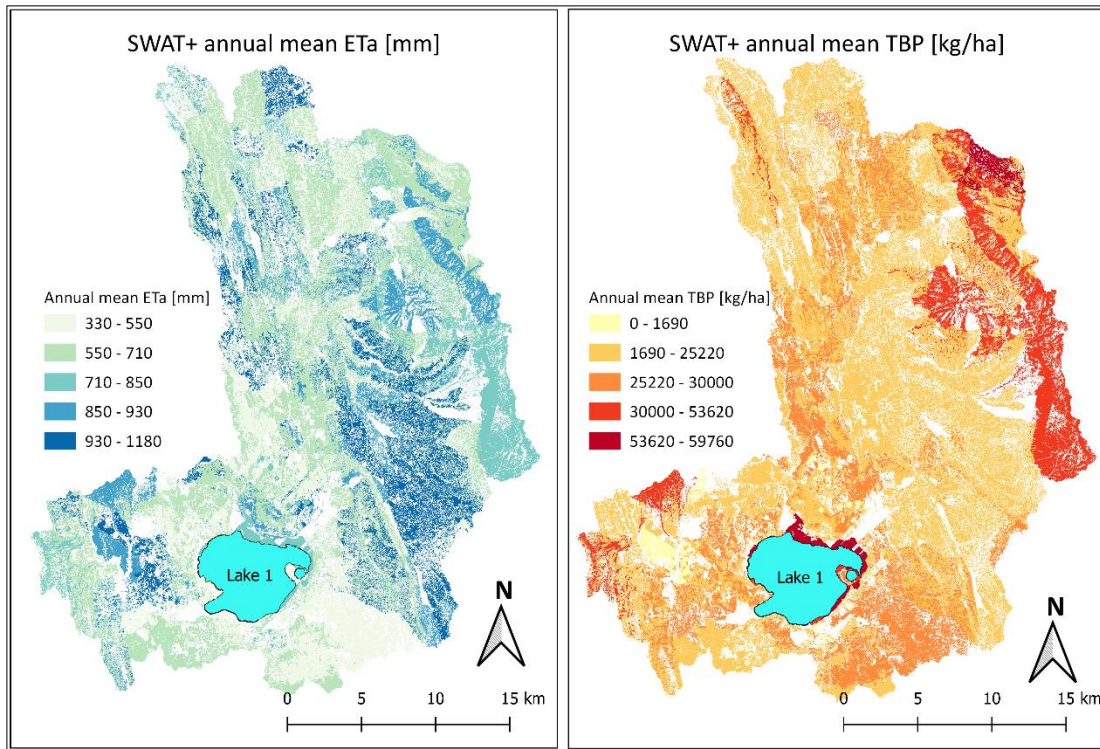


Figure 5.13 Visual representation of the simulated annual means ETa [mm] and TBP[kg/ha] of the catchment for the period 2009-2019

Table 5.7 lists the obtained average annual TBP, ETa, and TBWP for the entire catchment. These yearly TBP results further reflect the obtained monthly TBP (Figure 5.12) on less varying values.

Table 5.7 Average annual TBP, ETa, and TBWP obtained in the entire catchment

Year	TBP [kg/ha]	ETa [mm]	TBWP [kg/m³]
2009	31976.79	801.61	3.99
2010	31981.03	816.20	3.92
2011	31975.75	837.92	3.82
2012	31974.68	819.31	3.90
2013	31976.48	829.72	3.85
2014	31973.80	843.69	3.79
2015	31973.11	820.16	3.90
2016	31974.01	788.94	4.05
2017	31968.53	780.32	4.10
2018	31974.96	746.28	4.28
2019	31972.75	750.90	4.26
Mean	31974.72	800.20	3.99

The annual mean ETa [mm] was then converted to [m³/ha] by applying 1mm = 1L/m² = 10 m³/ha in order to calculate the TBWP [kg/m³]. An average annual TBP, ETa and TBWP of 31974.72 kg/ha, 800.20 mm and 3.99 kg/m³ respectively were eventually obtained.

5.7. Wheat and maize crop analysis

On assumption that crops have been growing on the same areas for the past 11 years, wheat and maize; yields, ETa and WP were analyzed in addition to the catchment-wide analysis. It was noted that the model TBP output in seasonal and annual crops differed at the different timesteps but perennial plants (forest, shrubland, grassland, and alfalfa) were well represented. This is evidenced with the represented values in ‘hru_pw_mon.txt’ and ‘hru_pw_yr.txt’ output files. Also, the model does not implement all calculations, and hence, the output generation on crop yields and land cover management is not fully available.

Crop information in Figure 4.4 was incorporated into the model as management practices. Wheat is planted in May and completely removed from the farm by a ‘harvest and kill’ operation in November. Maize is planted in April and ‘harvested and killed’ in December. Wheat and maize have 150 ‘days to maturity’ and 180 ‘days to maturity’ respectively. The crops were considered as rainfed, and other management practices including fertilizers application and pest control were not considered in this analysis.

The model simulates crop data at many HRUs; wheat and maize covering approximately 2776.85 ha and 394.01 ha respectively. Simulated yields for a few selected HRUs with the two crops were evaluated against Nyandarua county office obtained crop yields from farmers in the region (Figure 5.14). Wheat at HRU 1584 and HRU 1621 at the Kijabe farm area, and maize at HRU 1614 (downstream area of the catchment) and HRU 257 (upstream area) were analyzed. By default, the model applies harvest indices of 0.42 and 0.5 for wheat and maize respectively (Neitsch et al., 2009).

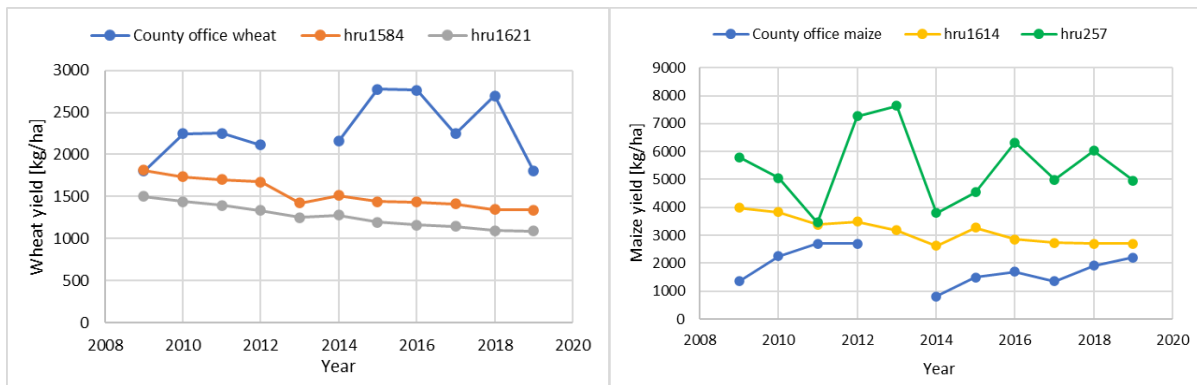


Figure 5.14 Wheat and maize yield from Nyandarua county office against SWAT+ simulations at specific HRUs

Srinivasan, Zhang, & Arnold (2010) recommended the evaluation of SWAT model average annual crop yields instead of crop yield at annual timestep, as the model is limited in accurate representation of crop data at higher timestep. This is also witnessed in this analysis (Figure 5.14), where the presented yield results don’t vary much across the year. However, maize at HRU 257 indicates some major fluctuations.

Figure 5.14 shows that the model simulates lower annual wheat yields (average of 1261.70 kg/ha/year and 1530.02 kg/ha/year at HRU 1621 and HRU 1584 respectively) than the county office (2286.26 kg/ha/year), but higher annual maize yield (average of 5444.46 kg/ha/year and 3159.07 kg/ha/year at HRU 257 and HRU 1614 respectively) than the county office (1846.90 kg/ha/year). The fact that the county crop data represents sampled information form farmers in Nyandarua county has a significant impact on the uncertainty in the above results.

COMPARISON OF WAPOR RS-BASED TO SWAT+ MODEL WATER PRODUCTIVITY IN LAKE NAIVASHA
BASIN, KENYA

The wheat and maize results at each year are listed in Table 5.8 and Table 5.9. The decrease in wheat and maize yields, apart from HRU 257, across the study period, reflect on the obtained decrease in WP results. For wheat, the average annual ETa at HRU 1621 and HRU 1584 were 560.45 mm and 563.07 mm respectively, and average annual maize ETa at HRU 257 and HRU 1614 were 833.69 mm and 788.06 mm respectively. The crops WP aspect was calculated in terms of grain yield per unit water use (ETa in this case). Average annual wheat WP of 0.23 kg/m³ and 0.27 kg/m³ were obtained at HRU 1621 and HRU 1584 respectively. While average annual maize WP of 0.65 kg/m³ and 0.40 kg/m³ were obtained at HRU 257 and HRU 1614 respectively, indicating that the WP for maize is larger than for wheat.

Table 5.8 Wheat crop WP simulated results

Wheat						
Year	HRU1621			HRU1584		
	Yield [kg/ha]	ETa [mm]	WP [kg/m ³]	Yield [kg/ha]	ETa [mm]	WP [kg/m ³]
2009	1501.55	562.98	0.27	1813.74	567.12	0.32
2010	1437.49	570.51	0.25	1735.96	573.57	0.30
2011	1393.23	539.86	0.26	1703.02	541.74	0.32
2012	1335.14	564.41	0.24	1674.92	566.15	0.30
2013	1248.24	562.86	0.22	1420.62	565.43	0.25
2014	1280.33	541.47	0.24	1512.53	544.11	0.28
2015	1196.37	538.49	0.22	1440.67	540.51	0.27
2016	1159.11	560.94	0.21	1432.72	562.17	0.26
2017	1143.66	571.71	0.20	1412.77	575.13	0.25
2018	1095.68	596.65	0.18	1344.39	598.90	0.23
2019	1087.91	555.06	0.20	1338.85	558.92	0.24
Mean	1261.70	560.45	0.23	1530.02	563.07	0.27

Table 5.9 Maize crop WP simulated results

Maize						
Year	HRU1614			HRU257		
	Yield [kg/ha]	ETa [mm]	WP [kg/m ³]	Yield [kg/ha]	ETa [mm]	WP [kg/m ³]
2009	3988.96	827.51	0.48	5800.71	832.11	0.70
2010	3824.01	784.90	0.49	5052.42	830.05	0.61
2011	3375.42	743.36	0.45	3463.07	828.23	0.42
2012	3484.19	781.98	0.45	7268.84	828.11	0.88
2013	3184.14	777.97	0.41	7642.20	846.51	0.90
2014	2624.78	764.59	0.34	3807.48	799.35	0.48
2015	3272.06	791.71	0.41	4541.57	824.44	0.55
2016	2859.71	767.02	0.37	6323.92	854.34	0.74
2017	2734.95	812.27	0.34	4996.96	841.75	0.59
2018	2706.13	837.23	0.32	6035.44	842.65	0.72
2019	2695.43	780.16	0.35	4956.44	843.08	0.59
Mean	3159.07	788.06	0.40	5444.46	833.69	0.65

6. WAPOR WATER PRODUCTIVITY ANALYSIS

6.1. Methodological approach

WaPOR time series data sets can be accessed via the FAO WaPOR website, but were also provided by the consortium to the ITC server (FAO, 2020). The FAO-Frame toolbox in ILWIS (Westen et al., 2001) was created to process WaPOR data. This research focused on Version II of the Level II product for Lake Naivasha basin in Kenya. 2009-2019 time series data sets at dekadal time-step were provided. These include evaporation, transpiration, interception and net primary production listed in Table 6.1.

Table 6.1 Provided WaPOR Level II datasets used for Lake Naivasha basin in this study.

Dataset	Timestep	Start date	End date	Scaling	Units
Evaporation	dekad	01/01/2009	31/12/2019	10	[mm/day]
Interception	dekad	01/01/2009	31/12/2019	10	[mm/day]
NPP	dekad	01/01/2009	31/12/2019	1000	[gC/m ² /day]
Transpiration	dekad	01/01/2009	31/12/2019	10	[avg mm/day]

Scripts that facilitate the data processing were provided in the ILWIS FAO-Frame toolbox and could be edited based on user-defined goals. The data processes could either be conducted by editing the codes generated on ILWIS command line or by using external batch routine processes in MS-DOS. Following the procedure in Maathuis (2019), ETI_a¹, TBP and TBWP on dekadal basis were calculated by implementing respective scripts repeatedly taking into consideration the number of days per dekad. The equations are as shown below.

i. ETI_a calculation

$$ETI_a = \frac{E + T + I}{10} * N \quad \text{Equation 6.1}$$

where E, T, and I are daily evaporation [mm], transpiration [mm] and interception [mm] respectively, 10 is the scaling factor, and N is the number of days per dekad. ETI_a units are in [mm/dekad] and can be converted into volume per unit area using; 1mm = 1L/m² = 10 m³/ha.

ii. TBP calculation

$$TBP = \frac{NPP * 22.222}{1000} * N \quad \text{Equation 6.2}$$

where TBP is the total biomass production [kg/ha] and N is the number of days per dekad. NPP is the net primary production [gC/m²/day], which is converted to dry matter production (DMP [kgDM/ha/day]) using a scaling factor of 0.45 gC/gDM (FAO, 2018). Thus, 1 NPP [gC/m²/day] is equal to 22.222 DMP [kgDM/ha/day]. 1000 is the scaling conversion factor.

¹ ETI_a [mm] represents ET_a [mm] in WaPOR analyses

iii. **TBWP calculation**

$$TBWP = \frac{TBP}{ETIa} \quad \text{Equation 6.3}$$

where TBWP [kg/m³] is the total biomass water productivity in a dekad, TBP [kg/ha/dekad] is the total biomass production, and ETIa [m³/ha/dekad] is the actual evapotranspiration and interception per dekad.

NPP values less than 0 were masked out. These areas are often waterbodies and greenhouses classified in the land cover maps, which result in ambiguous values in ETIa and TBP calculations. The processed datasets, from the provided defined window with bounding coordinates, were clipped to the Lake Naivasha basin polygon. Due to the large number of files generated, a comprehensive structure with consistent file naming was highly maintained as well as creating maplists in ILWIS.

6.2. Results analysis at yearly basis

The obtained dekadal time series results were aggregated to an annual basis by summing the 36 dekads in a year. The annual maps were averaged to mean annual data sets for the entire period. Yearly TBP, ETa and TBWP derived data components covering the entire catchment were evaluated by visual inspection on the raster maps and geographically averaged statistics over the catchment. These statistics include maximum, minimum, means and standard deviation.

$$Mean = \sum \frac{xi}{N} \quad \text{Equation 6.4}$$

$$SD = \sqrt{\frac{\sum(Xi - \bar{x})^2}{N}} \quad \text{Equation 6.5}$$

Where SD is the standard deviation xi is each value obtained, N is number of recorded data, and \bar{x} is the mean value.

6.2.1. ETa [mm/year]

Table 6.2 shows that the maximum and minimum ETa [mm/year] values per year differed across the study period. Year 2009 recorded the greatest range with 1808.2 mm/year. This could imply that there was greater variation in factors such as precipitation and land cover influencing ETa. In addition to this, a standard deviation of 318.0 mm/year was captured, indicating a greater difference of ETa values from the mean ETa value compared to the other years. Overall maximum and minimum ETa are 1514.6 mm/year and 226.4 mm/year respectively, the mean is 823.6 mm/year and the standard deviation is 214.1 mm/year for the entire catchment across the study period.

COMPARISON OF WAPOR RS-BASED TO SWAT+ MODEL WATER PRODUCTIVITY IN LAKE NAIVASHA
BASIN, KENYA

Table 6.2 Yearly statistics of WaPOR ETa [mm/year] (2009-2019) over the catchment.

	2009	2010	2011	2012	2013	2014	2015	2016	2017	2018	2019
Minimum	123.5	125.6	144.4	155	141.3	119.3	76.3	60.2	55.4	80.9	195.1
Maximum	1931.7	1794.0	1822.9	1781.4	1869.1	1388.4	1380.3	1351.8	1561.9	1415.9	1591.3
Mean	821.71	1023.41	957.6	981.21	1001.1	699.21	670.44	716.75	657.49	719.13	802.05
Sd	318.0	284.1	281.9	256.8	294.9	207.0	180.3	191.8	201.0	199.8	191.0

Figure 6.1 shows the yearly spatial variation in ETa [mm/year] in the catchment across the study period (2009-2019). It can be seen that the wetland areas around lake Naivasha as well as high altitude (forested) areas at Aberdare ranges and Mau Escarpment consistently have the high ETa over the years. The high ETa at the wetland areas is influenced by water surfaces which are greatly evaporated. The fact that forested areas captured high ETa could imply that intercepted precipitation by the canopy greatly contributes to the total ETa. The area north of the lake, which majorly consist of irrigation cropland areas, also shows a consistently high ETa in all the years. The far north-eastern and southern part of the catchment indicate low ETa as they consist of majorly bare rocks and dry shrubland covers.

Whereas the above discussed areas tend to limitedly vary throughout the years, the other parts of the catchment varied significantly. This could be explained by the heterogeneity in land covers. Generally, the yearly means recorded in Table 6.2 are reflected on the maps across the study period. Years 2009 to 2013 seem to show high ETa than years 2014 to 2019, though 2009 shows lower ETa (mean of 821.71 mm) among the first half study period, and 2019 shows higher ETa (mean of 802.05 mm) among the second half study period.

It was also noted that the years 2018 and 2019 show more masked out areas of waterbodies and greenhouses, as they appeared to have been captured in the respective land cover maps, compared to the other years.

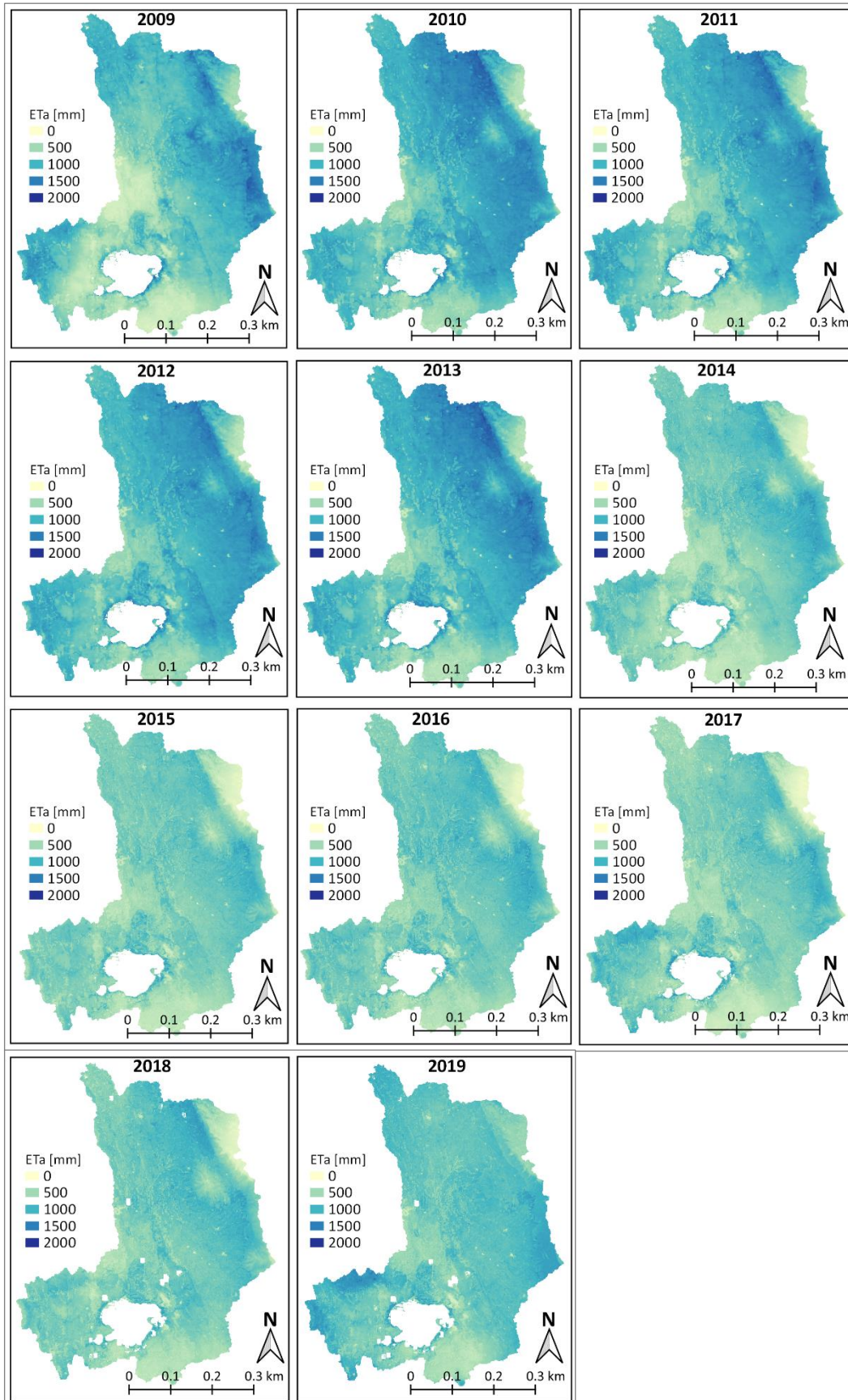


Figure 6.1 Yearly spatial distribution of WaPOR ETa [mm/year] in Lake Naivasha basin across the study period (2009-2019).

COMPARISON OF WAPOR RS-BASED TO SWAT+ MODEL WATER PRODUCTIVITY IN LAKE NAIVASHA
BASIN, KENYA

6.2.2. TBP [kg/ha/year]

Table 6.3 indicates that a minimum TBP of as low as 0 kg/ha/year was recorded in the specific years. Overall maximum and minimum TBP are 41241.2 kg/ha/year and 1873.4 kg/ha/year respectively, the mean is 23723.45 kg/ha/year and the standard deviation is 5174.7 kg/ha/year for the entire catchment across the study period.

Table 6.3 Yearly statistics of WaPOR TBP [kg/ha/year] (2009-2019) over the catchment.

	2009	2010	2011	2012	2013	2014	2015	2016	2017	2018	2019
Minimum	0.0	2389.2	1949.4	2180.9	2458.2	414.4	10.5	0.0	0.0	0.0	0.0
Maximum	43421.1	43034.5	42167.5	45714.3	49816.6	48019.5	46344.6	46199.4	48187.4	44705.0	50391.9
Mean	19160.9	26601.4	24418.2	25159.7	26946.8	22582.8	22226.8	24985.4	21146.1	23047.0	24252.4
Sd	7217.4	5206.2	5782.3	5294.7	5949.4	5460.3	5272.3	5546.2	6106.0	5155.8	5555.9

Figure 6.2 shows the yearly spatial variation of TBP [kg/ha/year] in the catchment across the study period (2009-2019). Wetland areas around lake Naivasha as well as the area north of the lake, which majorly consist of irrigation cropland areas, shows a consistently high TBP in all the years. The high TBP at the irrigated areas agree with the high ETa results (Figure 6.1), and could imply that sufficient water is applied for the high production of crop biomass. The Mau Escarpment and Aberdare ranges also shows high TBP over the years due to the perennial dense vegetation.

The far north-eastern and southern part of the catchment shows low TBP over the years. Results in this areas, coincide with the low ETa in Figure 6.1, as these areas consist of bare rocks and dry shrubland covers. Year 2009, with the lowest mean of 19160.9 kg/ha/year across the study period, shows that many areas in catchment reflect low TBP. The years 2018 and 2019 show more masked out areas of waterbodies and greenhouses, as they appeared to have been captured in the respective land cover maps, compared to the other years.

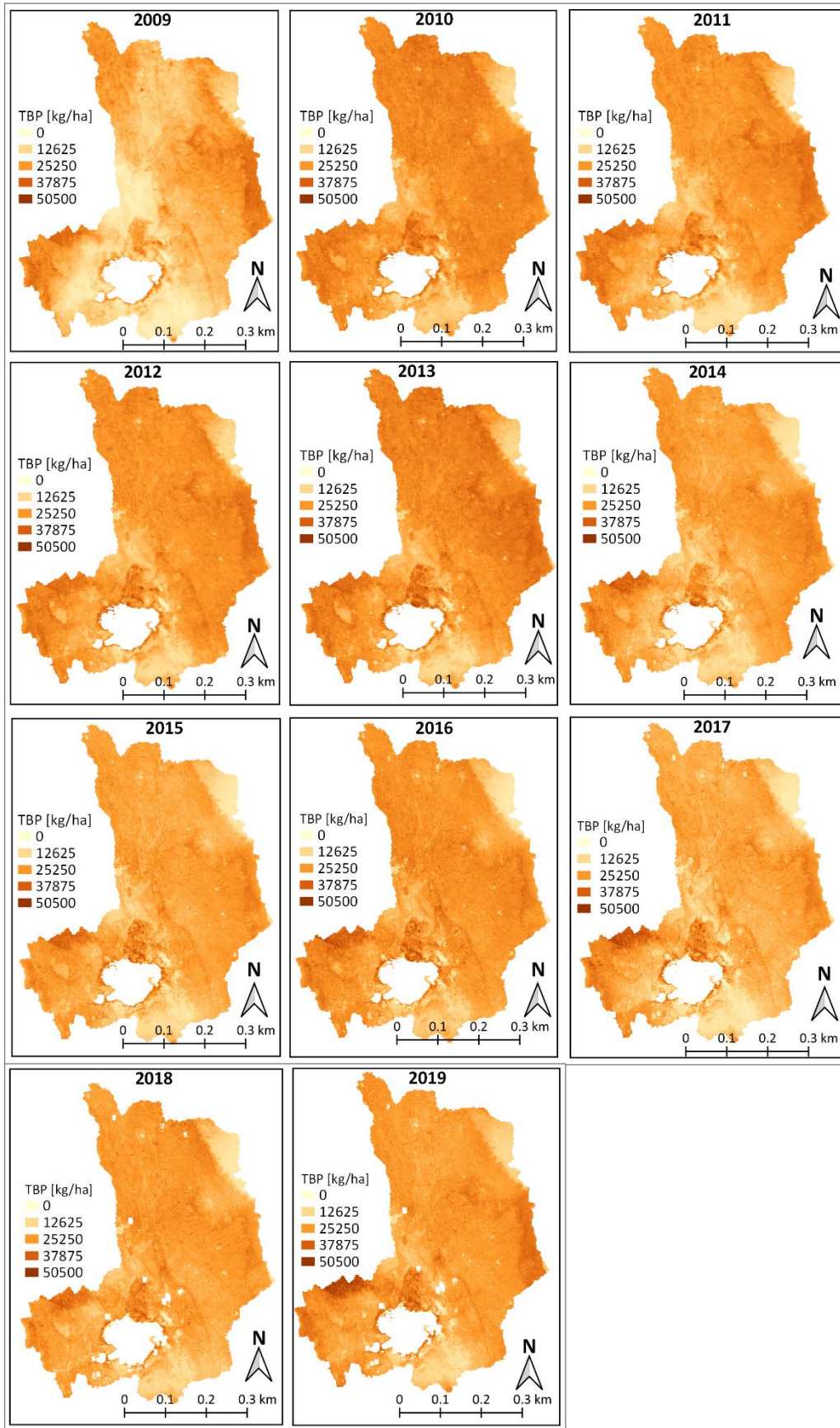


Figure 6.2 Yearly spatial distribution of WaPOR TBP [kg/ha] in Lake Naivasha basin across the study period (2009-2019).

COMPARISON OF WAPOR RS-BASED TO SWAT+ MODEL WATER PRODUCTIVITY IN LAKE NAIVASHA
BASIN, KENYA

6.2.3. TBWP [kg/m³]

Table 6.3 indicates that minimum TBWP values are as low as 0 kg/m³, while the maximum values vary across the study period. Overall maximum and minimum TBWP are 12.66 kg/m³ and 0.57 kg/m³ respectively, the mean is 3.02 kg/m³ and the standard deviation is 0.50 kg/m³ for the entire catchment across the study period. Years 2009-2013 recorded low TBWP values (mean of less than 3 kg/m³), while years 2014-2019 recorded higher TBWP values (mean of more than 3 kg/m³).

Table 6.4 Yearly statistics of WaPOR TBWP [kg/m³] (2009-2019) over the catchment.

	2009	2010	2011	2012	2013	2014	2015	2016	2017	2018	2019
Minimum	0.10	0.40	0.48	0.50	0.28	0.10	0.10	0.10	0.10	0.00	0.00
Maximum	13.60	22.80	18.83	16.60	18.19	11.80	10.20	10.70	12.30	11.00	6.06
Mean	2.39	2.71	2.64	2.64	2.80	3.33	3.40	3.60	3.31	3.31	3.05
Sd	0.49	0.58	0.54	0.52	0.55	0.58	0.62	0.71	0.73	0.63	0.41

Figure 6.3 shows the yearly spatial variation of TBWP in the catchment across the study period (2009-2019). It was noted that the far north-eastern and southern parts of the catchment, which consist of bare rocks and dry shrubland covers, show high TBWP across the study period. These areas recorded low ETa and TBP. The years 2018 and 2019 show more masked out areas of waterbodies and greenhouses, as they appeared to have been captured in the respective land cover maps, compared to the other years.

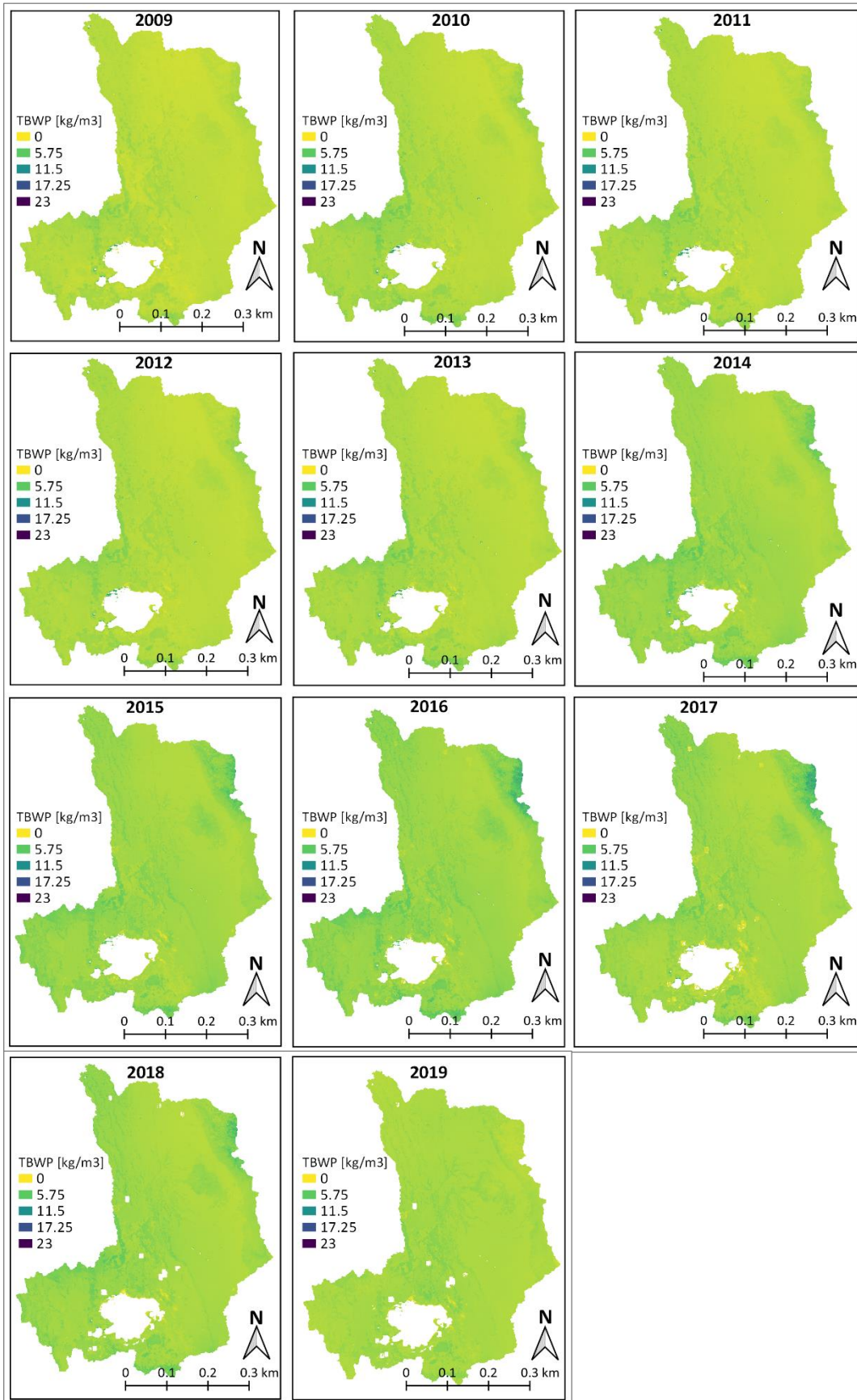


Figure 6.3 Yearly spatial distribution of WaPOR TBWP [kg/m³] in Lake Naivasha basin across the study period (2009-2019)

6.3. Results analysis at dekadal timestep

With an aim to capture the seasonal trend of WaPOR WP across the 11 years period for the entire catchment, the ETa, TBP and TBWP were analyzed at dekadal timestep. These were represented in time series graphs. The relationship between the TBP and ETa components at dekadal timestep was also reported.

Figure 6.4 indicates an irregular pattern with a high fluctuating trend across the time frame for both TBP and ETa. TBP shows a consistent lower trough of almost 200 kg/ha/dekad at the end of the first quartile (February-March) of every year, apart from 2013 and 2014 which record 400 kg/ha/dekad. These drops clearly indicate the dry season in the catchment. A high peak of 1000 kg/ha/dekad is measured in January 2010. A mean of 529.97 kg/ha/dekad was recorded across the time frame. The TBP relates positively to ETa with R^2 of 0.64.

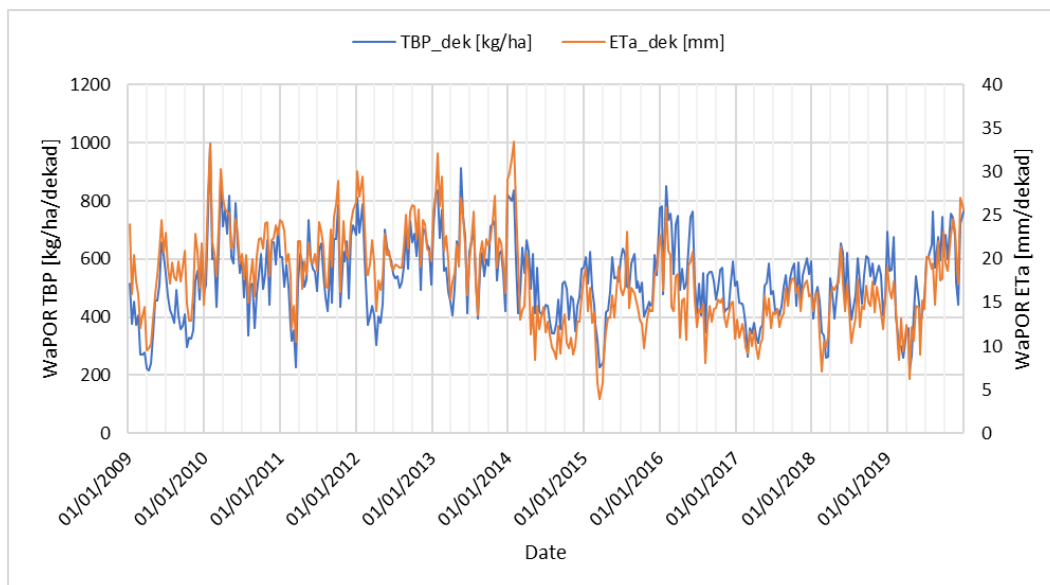


Figure 6.4 Time series representation of ETa [mm/dekad] and TBP [kg/ha/dekad] for years 2009-2019

A mean ETa of 17.57 mm/dekad was measured in the study period. The ETa highly fluctuates (Figure 6.4), but it was noted that 15-30 mm/dekad was measured in the first half (years 2009 to 2013) and then there was a decrease to approximately 5-25 mm/dekad in the second half (years 2014 to 2019). This is reflected in the TBWP graph (Figure 6.5) as ETa varies inversely to TBWP (Equation 6.3).

The decline in ETa from year 2014 to 2019 could imply that there was a reduction in precipitation which led to a reduction in soil moisture. Funk, Davenport, & Michaelsen (2010) reported that, due to climate change, there has been a continuous decrease in precipitation in Kenya in year 1960-2009, accompanied by increase in air temperature, which is expected by the year 2025 especially for regions which receive more than 100 mm during the long rains seasons.

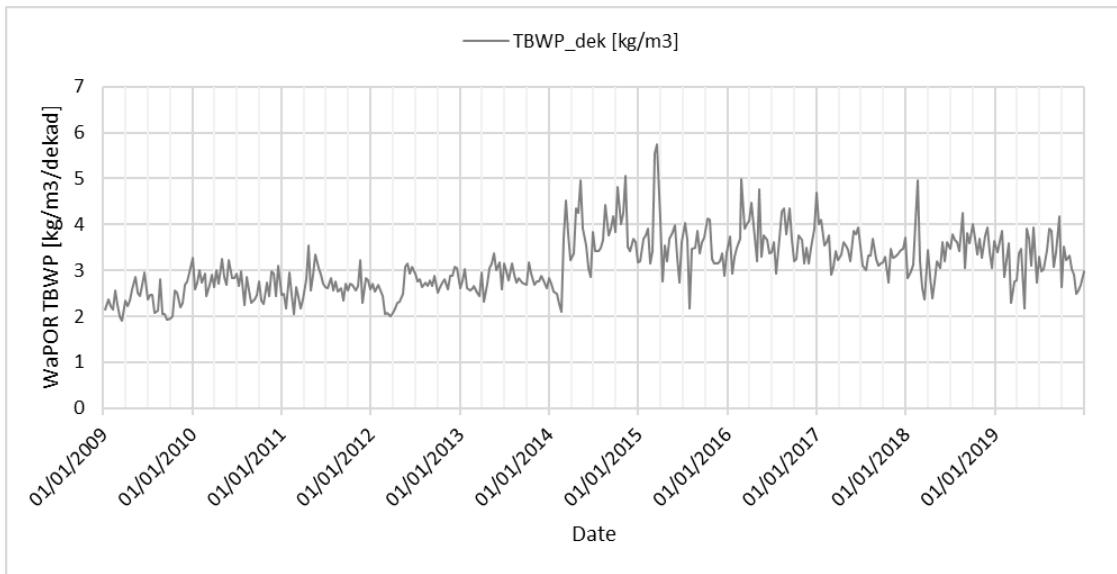


Figure 6.5 Time series representation of TBWP [kg/m³ at dekadal time-step

Figure 6.5 shows a fluctuating TBWP with a range of approximately 2-3 kg/m³ in the first half (years 2009 to 2013) and 2-5 kg/m³ in the second half (years 2014 to 2019). In dry seasons, where the ETa has lower values (troughs), the TBWP recorded high values (peaks). This indicates that the ETa decreases in the dry season, but the TBP is maintained relatively at the same level.

6.4. Wheat and maize crop results analysis

On assumption that the wheat and maize crops have been growing on the same farm areas for the past 11 years, the crops TBWP (Table 6.5) was analyzed at yearly basis, in addition to the overall catchment TBWP analysis. Wheat at Kijabe farm and maize at some parts of the upstream and downstream of the catchment gave average annual TBWP of 2.98 kg/m³ and 2.92 kg/m³ respectively. Wheat recorded lower TBP and ETa of 23160.74 kg/ha/year and 779.07 mm/year respectively, than maize, which recorded TBP of 2418.52 kg/ha/year and ETa of 836.24 07mm/year. The average annual wheat TBP and ETa are lower than maize, and this can be explained by the difference in structure of both plants.

The decrease in ETa in the second half period (2014-2019) (as it was seen from the overall catchment results in Figure 6.4 is also reflected in these crops. This is hence reflected in the TBWP results, where higher values are recorded in the second half period compared to the first half (2009-2013). However, lower maize ETa is recorded in year 2009. This could imply that in perhaps not the exact crop that was on site in that particular year, in reality. Results on that same year show the lowest TBWP of 2.51 kg/m³ and 2.39 kg/m³ at both wheat and maize respectively.

COMPARISON OF WAPOR RS-BASED TO SWAT+ MODEL WATER PRODUCTIVITY IN LAKE NAIVASHA
BASIN, KENYA

Table 6.5 Mean annual wheat ETa, TBP and TBWP across the 2009-2019 period.

Year	ETa [mm/year]		TBP [kg/ha/year]		TBWP [kg/m3]	
	Wheat	Maize	Wheat	Maize	Wheat	Maize
2009	812.38	744.70	20439.65	17790.49	2.51	2.39
2010	884.18	1021.88	25283.93	27012.80	2.85	2.79
2011	855.63	949.86	23990.23	24976.85	2.80	2.67
2012	862.67	960.93	23286.50	25393.74	2.68	2.69
2013	850.90	1022.38	24630.98	28464.26	2.88	2.84
2014	691.24	708.57	22740.73	22473.20	3.28	3.21
2015	685.96	773.10	22305.14	24507.46	3.25	3.16
2016	738.67	780.75	25408.54	25864.94	3.43	3.32
2017	774.69	745.04	22478.46	21325.73	2.90	2.86
2018	640.57	754.75	20704.64	23382.58	3.22	3.13
2019	772.87	736.68	23499.28	23011.74	3.04	3.13
Average	779.07	836.24	23160.74	24018.52	2.98	2.92

7. CONCLUSION AND RECOMMENDATION

7.1. Conclusion

The main objective of this research was to compare WaPOR Level II to SWAT+ model WP estimates in Lake Naivasha basin, Kenya, over an 11 years (2009-2019) study period. This thesis has demonstrated that WP estimated from the two approaches are comparable. The ultimate comparison results are presented at average annual basis, as the nature of datasets from these two approaches is different.

WaPOR WP estimates, based on ETa and TBP, are derived from satellite data sets and translated to dekadal and annual timesteps. SWAT+ on the other hand, is a hydrological model based on hydrological and plant growth processes which outputs the WP estimates based on ETa and TBP or crop yield. However, the temporal variability of the SWAT+ estimates was limited because of availability of the not so good nor complete long term in-situ meteorological data sets from stations in the study area. Therefore, CHIRPS precipitation and NCEP CFSR data together with the weather generator approach were adopted.

Ultimately, SWAT+ model gave an average annual WP of 3.99 kg/m³ compared to WaPOR which gave 3.02 kg/m³. TBP and ETa values of 23723.5 kg/ha/year and 823.6 mm/year were obtained from WaPOR, while SWAT+ gave TBP and ETa of 31974.7 kg/ha/year and 800.2 mm/year respectively.

In addition to the catchment-wide analysis, wheat and maize crops were analysed in both approaches. For WaPOR, the crops WP was estimated from TBP and ETa at the area covered by wheat and maize. For SWAT+, the crops WP were estimated from grain yield and ETa, with incorporated crop information collected from the fieldwork, at a few studied HRU levels. WaPOR gave average annual TBP, ETa and WP of 23160.74 kg/ha/year, 779.07 mm/year, and 2.98 kg/m³ respectively for wheat, and 24018.52 kg/ha/year, 836.24 mm/year, and 2.92 kg/m³ respectively for maize.

With SWAT+, wheat gave average annual ETa values of 560.45 mm/year and 563.07 mm/year at two HRUs studied (HRU 1621 and HRU 1584). Maize gave average annual ETa values of 833.69 mm/year and 788.06 mm/year (HRU 257 and HRU 1614). Average annual wheat crop yields of 1261.7 kg/ha/year and 1530.02 kg/ha/year were obtained. For maize yield, 5444.46 kg/ha/year and 3159.07 kg/ha/year were obtained. Therefore, wheat crop WP of 0.23 kg/m³ and 0.27 kg/m³, and maize crop WP of 0.65 kg/m³ and 0.40 kg/m³ were obtained.

In both WaPOR and SWAT+, maize gave higher ETa, TBP (for WaPOR) and crop yield (for SWAT+) estimates, than wheat. The crop WP results from both cases, however, differed. SWAT+ gave significantly higher maize WP than wheat, while WaPOR gave slightly higher wheat WP than maize.

7.2. Challenges and limitation

The main limitation in this research was the fact that the SWAT+ model version 1.3.0 is very new and has still several components under development, with limited documentation. This was a great hindrance especially in the anticipated calibration and validation processes.

Results of this study should caution users concerning SWAT+'s current capacity to accurately simulate biomass time series in a catchment. This limitation is evident in the outputs presented in yearly timestep.

Also, the model does not implement all calculations, and hence, the output generation on crop yields and land cover management is not fully available. For now, users are recommended to still fall back on the SWAT2012 or SWAT2018 models for this particular simulation.

The study area being located at the floor of the Rift Valley, with high altitudes at the Aberdare ranges in north-east and the Mau Escarpment at the west, gave a daily variation in the weather variables, thus a complex micro climatic conditions. Uncertainty in these weather data may highly have influenced the results regarding both WaPOR and SWAT+. For WaPOR ETa, for instance cloud cover is an influencing factor in the tropical climate. The adopted weather input data in SWAT+ model failed to capture the topographic difference and spatial heterogeneity in the study area, as they were derived from CHIRPS (precipitation) and NCEP CFSR (the other variables) satellite data.

7.3. Recommendations

Based on the research findings, it is recommended that input data quality, especially for the insitu weather data, for SWAT+, needs to be improved. This can be done by proper maintenance of the weather instruments in the field in order to function effectively. Another approach; is to investigate and apply downscaling techniques to obtain improved surface meteorological information. Research on this is ongoing by Njuki (current PhD research).

Also, performance of the established model for Lake Naivasha basin could be improved in the future by calibration and validation processes, for example with the newly developed SWATPlus CUP tool. The sensitivity analysis results obtained in this research could also be used as a starting point in these analyses. The model could also be improved by factoring in other farm management activities such as nutrient supply and control in water supply depending on the land cover.

For the WaPOR, it is recommended that evaluation of various data input quality including NDVI, albedo, cloud cover, and atmospheric conditions such as precipitation and temperature to be conducted to further explain the current results, as the quality and accuracy of the output is influenced by input data source. Also, Level III WP could be analyzed for the specific crop information collected in this research, such as at a specific irrigation or rainfed areas, then compared to the obtained level II results to check the consistency of the results.

LIST OF REFERENCES

- Abbasi, Y., Mannaerts, C. M., & Makau, W. (2019). Modeling pesticide and sediment transport in the Malewa River Basin (Kenya) using SWAT. *Water (Switzerland)*, 11(1), 1–20. <https://doi.org/10.3390/w11010087>
- Abbaspour, K. C. (2015). *SWAT-CUP: SWAT Calibration and Uncertainty Programs - A User Manual*. *eawag aquatic research*. Eawag: Swiss Federal Institute of Aquatic Science and Technology. Retrieved from https://swat.tamu.edu/media/114860/usermanual_swatcup.pdf
- Adimo, O. (2016). *Application of the GYGA approach to Kenya*. Nairobi. Retrieved from <http://www.yieldgap.org/kenya>
- Al-Sabbagh, M. (2001). *Surface runoff modelling using GIS and Remote Sensing. A case study in Malewa catchment, Naivasha, Kenya*. Enschede.
- Alemseged, T. (2002). *Explaining satellite-derived Actual evapotranspiration patterns In Homogeneously cropped large fields (Naivasha-Kenya)*. Enschede.
- Alila, P. O., & Atieno, R. (2006). Agricultural Policy in Kenya: Issues and Processes. In A. O. Shem (Ed.), *Future Agricultures Consortium workshop* (p. 41). Nairobi: Institute for Development Studies.
- Allen, R. G., Jensen, J. L., Wright, & Burman, R. D. (1989). Operational estimates of evapotranspiration. *Agron*, (81), 650–662.
- Armstrong, M. F. (2002). *Water Balance of the Southern Kenya Rift Valley Lakes*. MSc Thesis. Enschede. Retrieved from <ftp://ftp.itc.nl/pub/naivasha/ITC/Amstrong2002.pdf>
- Arnold, J. G., & Fohrer, N. (2005). SWAT2000: Current capabilities and research opportunities in applied watershed modelling. *Hydrological Processes*, 19(3), 563–572. <https://doi.org/10.1002/hyp.5611>
- Arnold, J. G., Kiniry, J. R., Srinivasan, R., Williams, J. R., Haney, E. B., & Neitsch, S. L. (2012). SOIL & WATER ASSESSMENT TOOL Input/Output Documentation Version 2012. In *TSoil and Water Assessment Tool "SWAT": Input/Output Documentation* (pp. 187–211). Texas: Texas Water Resources Institute. https://doi.org/10.1007/978-0-387-35973-1_1231
- Arnold, J. G., Kiniry, J. R., Srinivasan, R., Williams, J. R., Haney, E. B., & Neitsch, S. L. (2019). CHAPTER FILE.CIO SWAT+ INPUT DATA REVISED DOCUMENT, 59(2).
- Arnold, J. G., Moriasi, D. N., Gassman, P. W., Abbaspor, K. C., White, M. J., Srinivasan, R., ... Jha, M. K. (2012). SWAT: MODEL USE, CALIBRATION, AND VALIDATION. *American Society of Agricultural and Biological Engineers*, 55(4), 1491–1508.
- Bastiaanssen, W. G. M., Cheema, M. J. M., Immerzeel, W. W., & Miltenburg, I. J. (2012). Surface energy balance and actual evapotranspiration of the transboundary Indus Basin estimated from satellite measurements and the ETLook model. *WATER RESOURCES RESEARCH*, 48, 1–16. <https://doi.org/10.1029/2011WR010482>
- Becht, R., & Harper, D. M. (2002). Towards an understanding of human impact upon the hydrology of Lake Naivasha, Kenya. *Hydrobiologia*, 488, 1–11. <https://doi.org/10.1023/A:1023318007715>
- Becht, R., Odada, E., & Higgins, S. (2005). Lake Naivasha: experience and lessons learned brief. ... *Initiative: Experience and Lessons Learned Briefs* ..., 5, 22. Retrieved from <http://scholar.google.com/scholar?hl=en&btnG=Search&q=intitle:Lake+Naivasha+Experience+and+Lessons+Learned+Brief#0>
- Bieger, K., Arnold, J. G., Rathjens, H., White, M. J., Bosch, D. D., Allen, P. M., ... Srinivasan, R. (2017). Introduction to SWAT+, A Completely Restructured Version of the Soil and Water Assessment Tool. *Journal of the American Water Resources Association (JAWRA)*, 53(1), 115–130. <https://doi.org/10.1111/1752-1688.12482>
- Blatchford, M. (2016). *Developing a Water Productivity Target Framework. Case Study: West Bank, Palestine*. Delft.
- Blatchford, M., Mannaerts, C., Njuki, S., Nouri, H., Zeng, Y., Pelgrum, H., ... Karimi, P. (2019). Evaluation of WaPOR V2 . 0 evapotranspiration products across Africa. *Anthorea*, 1–24. <https://doi.org/10.22541/au.157541664.43295641>
- Cai, X., Thenkabail, P. S., Biradar, C. M., Platonov, B. A., Gumma, M., Dheeravath, V., ... Markandu, A. (2009). Water productivity mapping using remote sensing data of various resolutions to support “more crop per drop.” *Journal of Applied Remote Sensing*, 3(1), 24. <https://doi.org/10.1117/1.3257643>
- Cho, J., Bosch, D., Lowrance, R., Strickland, T., & Vellidis, G. (2009). Effect of spatial distribution of rainfall on temporal and spatial uncertainty of SWAT output. *Transactions of the ASABE*, 52(5), 1545–1555. <https://doi.org/10.13031/2013.29143>
- Clarke, M. C. G., Woodhall, D., Allen, D., & Darling, G. (1990). Geological, volcanological and hydrogeological controls on the occurrence of geothermal activity in the area surrounding Lake Naivasha, Kenya. Retrieved April 11, 2020, from <https://searchworks.stanford.edu/view/2245812>
- De Jong, T. (2011). *Water Abstraction Survey in Lake Naivasha Basin, Kenya*. Wageningen. Retrieved from https://www.academia.edu/1318847/de_Jong_2011_River_water_resource_monitoring_and_alloc

LIST OF REFERENCES

- tion_planning_Lake_Naivasha_basin_Kenya
- Defourny, P., Jarvis, I., & Blaes, X. (2014). *JECAM Guidelines for cropland and crop type definition and field data collection*. Retrieved from <http://jecam.org/>
- Dile, Y., Srinivasan, R., & George, C. (2015). *QGIS Interface for SWAT+: (QSWAT+). Setup for Robit Watershed, Lake Tana Basin*. <https://doi.org/10.13140/RG.2.1.1060.7201>
- Dile, Y. T., Daggupati, P., George, C., Srinivasan, R., & Arnold, J. (2016). Introducing a new open source GIS user interface for the SWAT model. *Environmental Modelling and Software*, *85*, 129–138. <https://doi.org/10.1016/j.envsoft.2016.08.004>
- Dinku, T., Funk, C., Peterson, P., Maidment, R., Tadesse, T., Gadain, H., & Ceccato, P. (2018). Validation of the CHIRPS satellite rainfall estimates over eastern Africa. *Quarterly Journal of the Royal Meteorological Society*, *144*(S1), 292–312. <https://doi.org/10.1002/qj.3244>
- eLEAF. (2020). *WaPOR Data Manual Evapotranspiration v2*. Wageningen. Retrieved from <http://www.eleaf.com>
- FAO. (2011). *Looking ahead in world food and agriculture: Perspectives to 2050*. (P. Conforti, Ed.). Rome: food and agriculture organization of the united nations. Retrieved from <http://www.fao.org/3/i2280e/i2280e.pdf>
- FAO. (2018). *Using remote sensing in support of solutions to reduce agricultural water productivity gaps. Database methodology: Level 2 data. WaPOR Version 1* (Vol. 1). Rome. Retrieved from <http://www.fao.org/in-action/remote-sensing-for-water-productivity/en/>
- FAO. (2019). *WaPOR Database methodology, V2 release*. Rome. Retrieved from www.fao.org/publications
- FAO. (2020). FAO Water Productivity. Retrieved June 1, 2020, from https://wapor.apps.fao.org/home/WAPOR_2/1
- Funk, C. (2018). Climate Hazard Group Releases New Version of CHIRPS, UCSB Geography. Retrieved July 4, 2020, from <https://geog.ucsb.edu/climate-hazard-group-releases-new-version-of-chirps/>
- Funk, Chris, Davenport, F., & Michaelsen, J. (2010). *A Climate Trend Analysis of Kenya—August 2010*. Retrieved from http://www.fews.net/docs/Publications/ke_fullmap_
- Google Earth. (n.d.). Google map Naivasha, kenya. Retrieved January 8, 2020, from <http://www.earth.google.com>
- Gorelick, N., Hancher, M., Dixon, M., Ilyushchenko, S., Thau, D., & Moore, R. (2017). Google Earth Engine: Planetary-scale geospatial analysis for everyone. <https://doi.org/10.1016/j.rse.2017.06.031>
- Green, H., & Ampt, G. A. (1912). Studies on soil physics: Part II — the permeability of an ideal soil to air and water. *The Journal of Agricultural Science*, *5*(1), 1–26. <https://doi.org/10.1017/S0021859600001751>
- Her, Y., Frankenberger, J., Chaubey, I., & Srinivasan, R. (2015). Threshold effects in HRU definition of the soil and water assessment tool. *Transactions of the ASABE*, *58*(2), 367–378. <https://doi.org/10.13031/trans.58.10805>
- ISRIC SOTER. (2010). ISRIC Soil Data Hub | ISRIC World Soil Information. Retrieved July 4, 2020, from <https://www.isric.org/explore/isric-soil-data-hub>
- Liu, B., & Gan, H. (2018). Evapotranspiration management based on the application of SWAT for balancing water consumption: A case study in Guantao, China. *Journal of Earth System Science*, *127*(51), 1–15. <https://doi.org/10.1007/s12040-018-0958-8>
- Liu, J., Zehnder, A. J. B., & Yang, H. (2008). Drops for crops: Modelling crop water productivity on a global scale. *Global Nest Journal*, *10*(3), 295–300. <https://doi.org/10.30955/gnj.000486>
- Lukman, A. P. (2003). *REGIONAL IMPACT OF CLIMATE CHANGE AND VARIABILITY ON WATER RESOURCES (CASE STUDY LAKE NAIVASHA BASIN, KENYA)*. Enschede.
- Maathuis, B. (2019). *FAO-FRAME Toolbox – Supporting calculation of Water Productivity*. Enschede.
- Macharia, P. N. (2004). Soil and Terrain Database for Kenya (KENSOTER), version 2.0, ISRIC Data Hub. <https://doi.org/ISO 19115:2003/19139>
- Makau, W. (2018). *Evaluation of Suspended Sediment Transport in the River Malewa Basin Using the Swat Model and Field Digital Turbidity Sensor Data*. Faculty of Geo-Information Science and Earth Observation of the University of Twente.
- Mannaerts, C., Blatchford, M., Njuki, S., Zeng, Y., Nouri, H., & Maathuis, B. (2020). *WaPOR V2 quality assessment, Technical report on the data quality of the WaPOR database version 2*. Enschede.
- Mannaerts, C., Blatchford, M., & Zeng, Y. (2018). *FRAME β -version Data Validation Report*. Enschede.
- Marek, G. W., Gowda, P. H., Evett, S. R., Baumhardt, R. L., Brauer, D. K., Howell, T. A., ... Srinivasan, R. (2015). Evaluation of SWAT for estimating ET in irrigated and dryland cropping systems in the Texas high plains. *Joint ASABE/LA Irrigation Symposium 2015: Emerging Technologies for Sustainable Irrigation*, *7004*, 1–15. <https://doi.org/10.13031/irrig.20152141855>
- McCarthy, G. (1938). *The Unit Hydrograph and Flood Routing Conf.* Noth Atlantic Div: New London,

LIST OF REFERENCES

- Conn.
- Meins, F. M. (2013). *Evaluation of spatial scale alternatives for hydrological modelling of the Lake Naivasha basin, Kenya*. MSc Thesis. Enschede.
- Ministry of Water and Irrigation. (2007). *REPUBLIC OF KENYA, The National Water Services Strategy (NWS)*. Nairobi.
- Mockus, V. (1972). USDA Soil Conservation Service. In V. Mckeever, W. Owen, & R. Rallison (Eds.), *National Engineering Handbook, Section 4*.
- Molden, D. (2007). Comprehensive Assessment of Water Management in Agriculture. *Water for Food, Water for Life: A Comprehensive Assessment of Water Management in Agriculture*. London, Earthscan, and Colombo: International Water Management Institute. <https://doi.org/10.4324/9781849773799>
- Molden, D., Murray-Rust, H., Sakthivadivel, R., & Makin, I. (2003). A water-productivity framework for understanding and action. *Water Productivity in Agriculture: Limits and Opportunities for Improvement*. Colombo: International Water Management Institute. <https://doi.org/10.1079/9780851996691.0001>
- Molden, D., Oweis, T. Y., Steduto, P., Kijne, J. W., Hanjra, M. A., & Bindraban, P. S. (2007). Pathways for increasing agricultural water productivity. In *Water use and productivity in a river basin* (pp. 279–310). International Water Management Institute.
- Monteith, J. L. (1965). Evaporation and Environment. *Symposia of the Society for Experimental Biology*, 19, 205–234.
- Monteith, J. L. (1972). *Solar Radiation and Productivity in Tropical Ecosystems*. *The Journal of Applied Ecology* (Vol. 9). <https://doi.org/10.2307/2401901>
- Moriasi, D. N., Arnold, J. G., Van Liew, M. W., Bingner, R. L., & Veith, T. L. (2007). MODEL EVALUATION GUIDELINES FOR SYSTEMATIC QUANTIFICATION OF ACCURACY IN WATERSHED SIMULATIONS. *American Society of Agricultural and Biological Engineers*, 50(3), 885–900.
- Mul, M., & Bastiaanssen, W. G. M. (2019). *WaPOR quality assessment: Technical report on the data quality of the WaPOR FAO database version 1.0*. Delft.
- Muthuwatta, L. P. (2004). *Long term Rainfall-runoff-lake level modelling of the lake Naivasha basin, Kenya*. MSc Thesis. Enschede. Retrieved from <http://citeseerx.ist.psu.edu/viewdoc/download?doi=10.1.1.2.3941&rep=rep1&type=pdf>
- Neitsch, S. L., Arnold, J. G., Kiniry, J. R., & Williams, J. R. (2005). SOIL AND WATER ASSESSMENT TOOL DOCUMENTATION VERSION 2005. Texas: GRASSLAND, SOIL AND WATER RESEARCH LABORATORY, AGRICULTURAL RESEARCH SERVICE.
- Neitsch, S. L., Arnold, J. G., Kiniry, J. R., & Williams, J. R. (2009). *Soil & Water Assessment Tool Theoretical Documentation Version 2009*. Texas Water Resources Institute. Texas. <https://doi.org/10.1016/j.scitotenv.2015.11.063>
- Njuki, S. M. (2016). *Assessment of Irrigation Performance by Remote Sensing in the Naivasha Basin, Kenya*. ITC MSc Thesis. Enschede.
- Ochieng, K. O. (2017). *Effect of Surface water abstractions on the inflow into Lake Naivasha (Kenya) using CREST model forced by earth observation based products*. Enschede. Retrieved from <https://www.itc.nl/library/research/academic-output/msc-theses/?year=2017&category=WREM>
- Odongo, V. O. (2016). *How climate and land use determine the hydrology of lake Naivasha basin*. University of Twente. <https://doi.org/10.3990/1.9789036542333>
- Pelgrum, H., Jehanzeb, M., & Cheema, M. (2010). ET Look: A novel continental evapotranspiration algorithm.
- Richardson, C. W., & Nicks, A. D. (1990). Weather Generator Description. In A. N. Sharpley & J. R. Williams (Eds.), *EPIC-Erosion/Productivity Impact Calculator* (pp. 93–104). U.S. Department of Agriculture Technical Bulletin.
- Ritchie, J. T. (1972). A Model for Predicting Evaporation From a Row Crop with Incomplete Cover. *Water Resources Research*, 8(5), 1–11. <https://doi.org/10.1029/WR008i005p01204>
- Ruimy, A., Kergoat, L., & Bondeau, A. (1999). Comparing global models of terrestrial net primary productivity (NPP): analysis of differences in light absorption and light-use efficiency. *Global Change Biology*, 5(S1), 56–64. <https://doi.org/10.1046/j.1365-2486.1999.00007>
- Sadras, V. O., Grassini, P., & Steduto, P. (2010). *Status of water use efficiency of main crops*. SOLAW Background Thematic Report TR07. Rome. Retrieved from http://www.fao.org/fileadmin/templates/solaw/files/thematic_reports/TR_07_web.pdf
- Saha, S., Moorthi, S., Pan, H. L., Wu, X., Wang, J., Nadiga, S., ... Goldberg, M. (2010). The NCEP climate forecast system reanalysis. Maryland: American Meteorological Society. <https://doi.org/10.1175/2010BAMS3001.1>
- Schuerz, C. (2019). SWATplusR: Running SWAT2012 and SWAT+ Projects in R.

LIST OF REFERENCES

- <https://doi.org/10.5281/zenodo.3373859>
- Sinnathamby, S., Douglas-Mankin, K. R., & Craige, C. (2017). Field-scale calibration of crop-yield parameters in the Soil and Water Assessment Tool (SWAT). *Agricultural Water Management*, 180, 61–69. <https://doi.org/10.1016/j.agwat.2016.10.024>
- SOFTWEL Pvt. (2020). SW Maps - GIS & Data Collector - Apps on Google Play. Retrieved May 28, 2020, from <https://play.google.com/store/apps/details?id=np.com.softwel.swmaps&hl=en>
- Sombroek, W. G., Braun, H. M. H., & van der Pouw, B. J. a. (1982). *Exploratory soil map and agro-climatic zone map of Kenya, 1980, scale 1:1,000,000*. Nairobi.
- Srinivasan, R., Zhang, X., & Arnold, J. (2010). SWAT ungauged: Hydrological budget and crop yield predictions in the upper Mississippi River basin. *American Society of Agricultural and Biological Engineers*, 53(5), 1533–1546. <https://doi.org/10.13031/2013.34903>
- Su, Z. (2002). The Surface Energy Balance System (SEBS) for estimation of turbulent heat fluxes. *Hydrology and Earth System Sciences*, 6(1), 85–100. <https://doi.org/10.5194/hess-6-85-2002>
- Tarboton, D. (2015). Terrain Analysis Using Digital Elevation Models (TauDEM) Version 5, Hydrology Research Group. Retrieved July 4, 2020, from <https://hydrology.usu.edu/taudem/taudem5/index.html>
- Tech, J. (2019). *SWAT+ Editor 1.2.0 Documentation*. Texas. Retrieved from plus.swat.tamu.edu
- Teixeira, A. H. C. (2008). *Measurements and modelling of evapotranspiration to assess agricultural water productivity in basins with changing land use patterns: a case study in the São Francisco River basin, Brazil*. Wageningen. Retrieved from <http://library.wur.nl/WebQuery/clc/1888476>
- Teshite, T. B. (2018). *Validation of Fao-Frame Remote Sensing Based Agricultural Water Productivity Estimates in the Upper Awash River*. ITC, Faculty of Geo-Information Science and Earth Observation, University of Twente.
- Texas Agriculture and Management University. (2020). Global weather for SWAT. NCEP Climate Forecast System Reanalysis (CFSR). Retrieved June 1, 2020, from <https://globalweather.tamu.edu/>
- Tiruneh, B. A. (2004). *Modeling Water Quality using Soil and Water Assessment Tool. A case study in Lake Naivasha Basin, Kenya*. Faculty of Geo-Information Science and Earth Observation, University of Twente.
- Tulshiram Thokal, R., Gorantiwar, S. D., Kothari, M., Bhakar, S. R., & Nandwana, B. P. (2015). Spatial Mapping of Agricultural Water Productivity Using the SWAT Model, 96(1), 85–98. <https://doi.org/10.1007/s40030-015-0113-3>
- USGS. (2018). USGS EROS Archive - Digital Elevation - Shuttle Radar Topography Mission (SRTM) 1 Arc-Second Global. <https://doi.org/10.5066/F7PRTFT>
- Vaghefi, S. A., Abbaspour, K. C., Faramarzi, M., Srinivasan, R., & Arnold, J. G. (2017). Modeling crop water productivity using a coupled SWAT-MODSIM model. *Water (Switzerland)*, 9(3), 1–15. <https://doi.org/10.3390/w9030157>
- Valentini, R. (2003). Fluxes of Carbon, Water and Energy of European Forests. *Springer Science & Business Media*, 163. Retrieved from <https://www.springer.com/gp/book/9783540437918>
- Westen, C. van, Farifteh, J., Maathuis, B., Huurneman, G., Meer, van der, F., & van Dijk, P. (2001). *Ihvis 3.0 Academic User's Guide*. Enschede.
- Williams, J. R. (1969). Flood Routing With Variable Travel Time or Variable Storage Coefficients. *Transactions of the ASAE*, 12(1), 100–103. <https://doi.org/10.13031/2013.38772>
- Winchell, M., Srinivasan, R., Di Luzio, M., & Arnold, J. (2010). *ArcSWAT interface for SWAT2009 User's Guide. User's guide*. Texas.
- Yen, H., Park, S., Arnold, J. G., Srinivasan, R., Chawanda, C. J., Wang, R., ... Zhang, X. (2019). IPEAT+: A Built-In Optimization and Automatic Calibration Tool of SWAT+. *Water*, 11(8), 1681. <https://doi.org/10.3390/w11081681>
- Zhang, Q., Singh, B., Gagnon, S., Rousselle, J., Evora, N., & Weyman, S. (2004). The Application of WGEN to Simulate Daily Climatic Data for Several Canadian Stations. *Canadian Water Resources Journal*, 29(1), 59–72.
- Zwart, S. J., & Bastiaanssen, W. G. M. (2004). Review of measured crop water productivity values for irrigated wheat, rice, cotton and maize. *Agricultural Water Management*, 69(2), 115–133. <https://doi.org/10.1016/j.agwat.2004.04.007>

APPENDIX A

Data	Purpose
Identified farm field, coordinates	Identification of the croplands locations
Size area of farmland	
Crop name, type of crop	Seasonal or annual
No. of crops (stems/seeds) or area planted	To determine the yield (productive stems)
No. of crops (stems/seeds) or area harvested	No. of plants per unit area
Single type of cropping or 2 types (which crops) or crop rotation	
Crop phenology information	
Tillage Methods	That facilitate soil holding capacity
Dates of development:	To establish crop calendar.
Planting	And thus determine days to maturity which derive heat units
Emergence	
Flowering	
Maturity	
Harvest	
Canopy height, and Root depth at minimum (emergence) and maximum (maturity) stage	Crop specific characteristics
Rainfed or irrigated	To validate irrigated and rainfed lands according to land cover map.
If irrigated: type of irrigation	
Dates, frequency, duration, timeliness and rate	To related irrigation method (if irrigating) to water productivity
Fertilizer application:	Land management practice that affect the yield
Which ones; N, P, K, organic (manure) other	
How much? (per day/per annum)	
At what stages of application	
Pest diseases and weed management	Land management practice that affect the yield
Which methods	
Runoff erosion occurrence?	Land management practice that affect the yield
Prevention techniques	

Questionnaire information on the collected crop data

Year	Maize yield			Wheat yield		
	Area [ha]	Production [ton]	[ton/ha]	Area [ha]	Production [ton]	[ton/ha]
2009	17850	24097.5	1.35	3670	6606	1.8
2010	18000	40500	2.25	2870	6457.5	2.25
2011	20352	54950.6	2.70001	2157	4854.8	2.250719
2012	19842	53574.6	2.70006	2034	4296.5	2.11234
2013	-	-	-	-	-	-
2014	17104	14017	0.819516	2097	4521	2.155937
2015	17837	26575.5	1.489909	4250	11813.04	2.779539
2016	16300	27594	1.692883	3520	9729	2.76392
2017	16200	21870	1.35	3800	8550	2.25
2018	17885	34289	1.917193	3560	9612	2.7
2019	16,906	37,184	2.199456	3572	6430	1.800112

Wheat and maize yield information in years 2009 to 2019, but missing 2013.

APPENDIX A

Crop	Planting ² [days]	Emergence [days]	Flowering [days]	Maturity [days]	Harvesting [days]
Baby corn	0	7	60	90	90
Normal corn	0	7	120 to 150	180 to 240	330 to 360
Wheat	0	4 to 5	130	140	140 to 160
Barley	0	7	42 to 45	120 to 150	175
Oats	0	8 to 10	45	120 to 150	120 to 150
French beans	0	7 to 10	35	75	90
Garden peas	0	7 to 14	50 to 60	75 to 80	120
Irish potatoes	0	30	60	120	150
Cabbages	Transplanted at 28 to 42 days old	-	-	60	60 to 90
Broccoli	Transplanted at 21 days old	-	60	70 to 80	90
Lucerne fodder	0	21	30	30 to 40	30 to 40

Crops phenology per growth stage; planting, emergence, flowering, maturity and harvesting for year 2019-2020 obtained during the fieldwork.



Different varieties of oats illustrated by the growth height (left) and appearance (right).

² Note: Emergence, flowering, maturity and harvesting days are counted from planting day that is day 0

APPENDIX A

①

Field data collection: Lake Naivasha basin, Kenya. Date:

1.	Location	Paul's Farm (06024°S 36.56653°E)
2.	Size area of farm land	1½ acres
3.	Crop (seasonal/annual)	Irish potatoes
4.	1/more types of cropping? crop rotation?	Yes, crop rotated with cabbages
5.	No. of crops/seeds planted (or area size)	6 bags in 1.5 acres (1 bag = 50kg)
6.	No. of crops/grains harvested (or area)	80 bags in 1.5 acres (1 bag = 50kg)
7.	Dates of crop development: Tillage (methods) Planting Emergence Flowering Mid-season Maturity Harvest - human labour	Tractor - machinery 01-09-2019 1 month after planting. (soil added to cover up the tuber crop after emergence) 2 months " " 1 month after emergence 120-150 days after planting. 4 months " " - colour changes from green to yellow.
8.	Canopy height at emergence Canopy height at maturity stage	@ 2cm from ground level. 30-40cm
9.	Root depth at emergence Root depth at maturity	2cm N/A; Roots grow horizontally more than vertically. 10-15cm
10.	Irrigation? (y/n) Type of irrigation Dates Frequency Duration Rate	N/A Rainfed.
11.	Fertilizer application? At what stages of application N, P, K, organic (manure) other Amount? (per day/per year)	i) DAP - diammonium phosphate (too acidic) - commonly used for maize also - when planting; mixed with soil. 4 bags of fertilizer per 1.5 acres 1 bag = 50kg ii) NPK - 16%, 46%, 0% iii) Foliar fertilizer - promote flowers
12.	Pest diseases/weed management? Methods	- Human labour - weed removal. + Frost reduction.
13.	Erosion occurrence? Prevention techniques	- little occurrence Planted grass strips on edges - act as fodder & reduce erosion.

*Infrared spacing - 2m
" crop " - 30cm
depth of plant - 15cm*

canopy = root depth

At planting

cold climate - near altitude ranges

Example of a filled questionnaire, information collected from a farmer during the fieldwork.

APPENDIX B

basin_pw_mon.txt - Notepad

File Edit Format View Help

swatplus_lnb5				SWAT+	Sept 26 2019	MODULAR Rev 2019.60.1	lai	bioms	yield	residue	sol_tmp	strsw	strsa
jday	mon	day	yr	unit	gis_id	name	m**2/m**2	kg	kg	kg	degc	---	---
31	1	31	2009	1	1	swatplus_lnb5	1.337	31947.688	0.000	180.877	15.596	3.310	6.758
59	2	28	2009	1	1	swatplus_lnb5	1.337	31947.740	0.000	132.619	16.819	5.379	3.310
90	3	31	2009	1	1	swatplus_lnb5	1.346	31953.527	0.000	97.653	16.825	5.722	3.553
120	4	30	2009	1	1	swatplus_lnb5	1.433	31978.596	0.000	70.780	15.854	1.955	8.013
151	5	31	2009	1	1	swatplus_lnb5	2.396	31993.088	0.077	51.698	14.746	1.110	10.251
181	6	30	2009	1	1	swatplus_lnb5	2.473	31989.887	7.128	42.347	13.816	1.206	9.169
212	7	31	2009	1	1	swatplus_lnb5	2.415	31985.318	2.808	38.843	13.122	2.184	7.408
243	8	31	2009	1	1	swatplus_lnb5	2.206	31992.367	2.772	39.146	13.095	2.057	6.940
273	9	30	2009	1	1	swatplus_lnb5	1.851	32000.273	0.770	41.105	14.722	3.679	3.911
304	10	31	2009	1	1	swatplus_lnb5	1.550	32008.893	0.566	33.957	15.205	3.357	3.172
334	11	30	2009	1	1	swatplus_lnb5	1.392	31970.711	12.805	42.720	14.759	2.086	6.474
365	12	31	2009	1	1	swatplus_lnb5	1.352	31951.568	9.739	39.402	14.609	2.510	9.164
31	1	31	2010	1	1	swatplus_lnb5	1.516	31947.688	0.000	42.812	15.667	3.331	6.253
59	2	28	2010	1	1	swatplus_lnb5	1.516	31947.756	0.000	30.879	16.577	5.275	5.040
90	3	31	2010	1	1	swatplus_lnb5	1.526	31956.570	0.000	22.456	17.058	7.384	4.252
120	4	30	2010	1	1	swatplus_lnb5	1.630	31985.814	0.000	16.124	16.021	3.724	7.398
151	5	31	2010	1	1	swatplus_lnb5	2.582	32001.707	0.093	11.895	14.789	1.979	9.593
181	6	30	2010	1	1	swatplus_lnb5	2.650	31996.461	8.578	13.909	13.968	0.974	10.975
212	7	31	2010	1	1	swatplus_lnb5	2.589	31992.504	0.070	17.558	13.167	1.493	7.524
243	8	31	2010	1	1	swatplus_lnb5	2.371	32003.074	1.305	22.220	13.190	3.138	5.879
273	9	30	2010	1	1	swatplus_lnb5	2.015	32003.664	6.452	30.654	14.532	2.951	3.209
304	10	31	2010	1	1	swatplus_lnb5	1.724	32009.346	0.622	26.281	15.158	3.007	3.660
334	11	30	2010	1	1	swatplus_lnb5	1.574	31973.023	12.190	35.606	14.575	1.978	8.918
365	12	31	2010	1	1	swatplus_lnb5	1.499	31952.648	10.755	40.475	14.656	2.358	9.228
31	1	31	2011	1	1	swatplus_lnb5	1.381	31947.688	0.000	65.220	15.762	3.612	6.422
59	2	28	2011	1	1	swatplus_lnb5	1.381	31947.752	0.000	47.372	16.540	4.079	4.570
90	3	31	2011	1	1	swatplus_lnb5	1.390	31954.459	0.000	34.519	16.765	3.754	5.354
120	4	30	2011	1	1	swatplus_lnb5	1.461	31979.389	0.000	24.868	15.884	1.729	8.856
151	5	31	2011	1	1	swatplus_lnb5	2.463	31991.611	0.009	18.240	14.766	0.465	8.538
181	6	30	2011	1	1	swatplus_lnb5	2.517	31989.852	7.023	17.478	13.867	0.233	9.723
212	7	31	2011	1	1	swatplus_lnb5	2.458	31989.688	1.136	20.114	13.131	0.447	10.442
243	8	31	2011	1	1	swatplus_lnb5	2.248	31989.596	4.771	26.189	13.066	0.625	6.830
273	9	30	2011	1	1	swatplus_lnb5	1.890	31996.979	1.127	30.235	14.582	2.143	5.918
304	10	31	2011	1	1	swatplus_lnb5	1.595	32004.652	0.293	25.570	15.172	3.009	5.019
334	11	30	2011	1	1	swatplus_lnb5	1.442	31969.018	11.934	34.847	14.497	1.323	8.044
365	12	31	2011	1	1	swatplus_lnb5	1.393	31950.727	8.861	31.880	14.564	1.480	9.742
31	1	31	2012	1	1	swatplus_lnb5	1.486	31947.688	0.000	24.976	15.575	2.747	7.463
60	2	29	2012	1	1	swatplus_lnb5	1.486	31947.756	0.000	17.777	16.680	4.416	4.485
91	3	31	2012	1	1	swatplus_lnb5	1.496	31955.041	0.000	12.768	16.834	4.911	4.720
121	4	30	2012	1	1	swatplus_lnb5	1.571	31977.965	0.000	9.051	15.953	1.418	8.541
152	5	31	2012	1	1	swatplus_lnb5	2.591	31991.211	0.028	6.714	14.836	0.622	9.542
182	6	30	2012	1	1	swatplus_lnb5	2.622	31988.379	7.707	9.289	13.859	0.745	9.689
213	7	31	2012	1	1	swatplus_lnb5	2.561	31984.158	0.363	14.273	13.064	1.728	8.346
244	8	31	2012	1	1	swatplus_lnb5	2.342	31991.215	4.889	20.897	13.342	2.229	5.581

Results on the monthly simulated TBP results over the entire catchment.

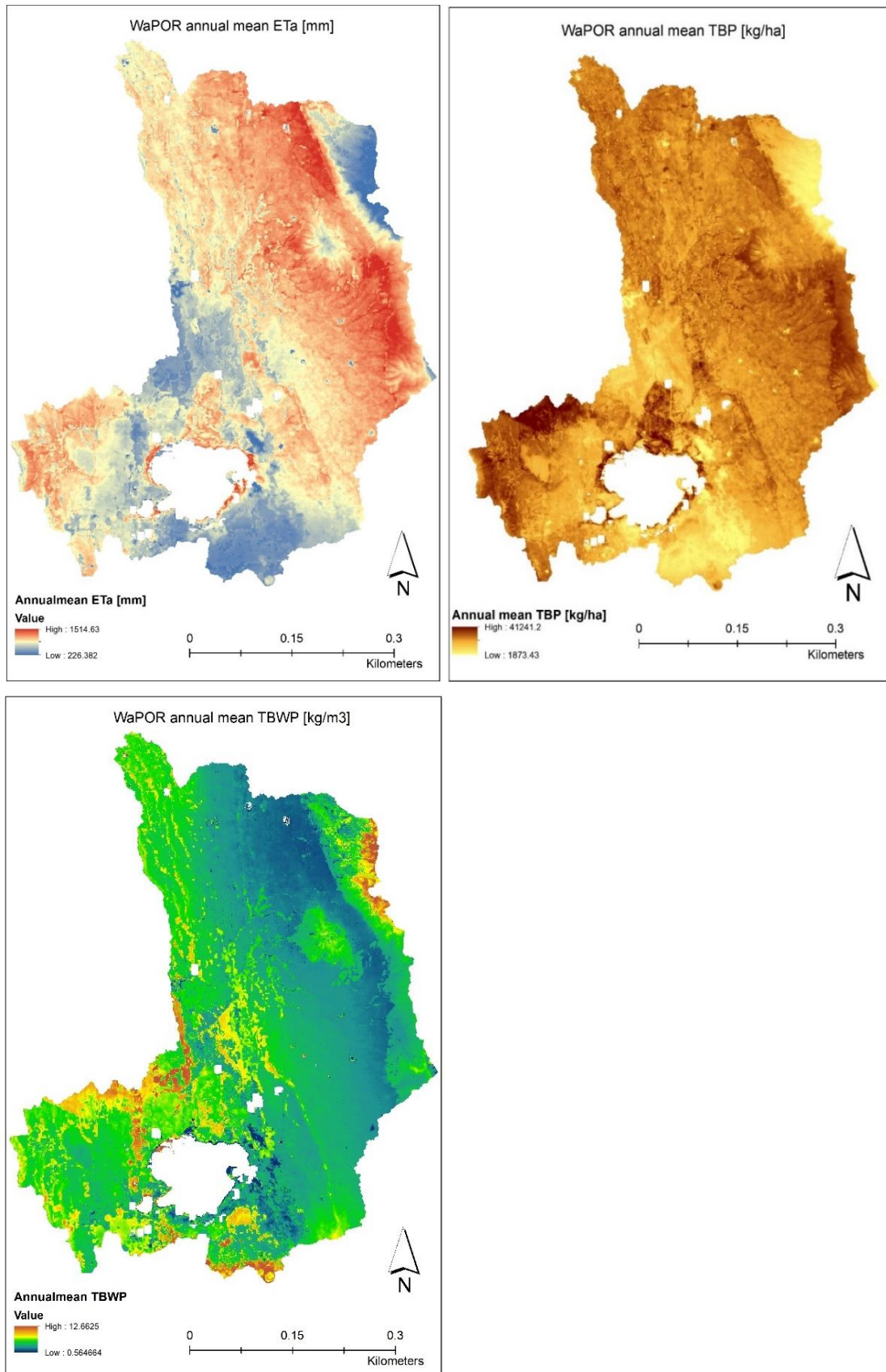
basin_pw_yr.txt - Notepad

File Edit Format View Help

swatplus_lnb5				SWAT+	Sept 26 2019	MODULAR Rev 2019.60.1	lai	bioms	yield	residue	sol_tmp	strsw
jday	mon	day	yr	unit	gis_id	name	m**2/m**2	kg	kg	kg	degc	---
365	12	31	2009	1	1	swatplus_lnb5	1.760	31976.787	36.665	67.263	14.917	34.556
365	12	31	2010	1	1	swatplus_lnb5	1.936	31981.029	40.063	25.885	14.935	37.592
365	12	31	2011	1	1	swatplus_lnb5	1.805	31975.754	35.155	31.296	14.871	22.898
366	12	31	2012	1	1	swatplus_lnb5	1.908	31974.684	34.252	19.633	14.917	29.128
365	12	31	2013	1	1	swatplus_lnb5	1.751	31976.477	34.272	34.355	14.908	28.863
365	12	31	2014	1	1	swatplus_lnb5	1.974	31973.797	32.339	21.540	14.883	24.791
365	12	31	2015	1	1	swatplus_lnb5	1.962	31973.107	31.917	18.978	14.919	33.112
366	12	31	2016	1	1	swatplus_lnb5	1.643	31974.006	35.454	44.693	14.922	29.869
365	12	31	2017	1	1	swatplus_lnb5	1.412	31968.529	27.361	36.022	14.901	26.072
365	12	31	2018	1	1	swatplus_lnb5	1.327	31974.961	32.969	55.148	14.904	31.396
365	12	31	2019	1	1	swatplus_lnb5	1.284	31972.746	30.066	43.226	14.920	29.592

Results on the yearly simulated TBP results over the entire catchment.

APPENDIX C



Average annual WaPOR ETa [mm] (a), TBP [kg/ha] (b) and TBWP [kg/m³] (c) for the study period.



River Malewa at upstream of Lake Naivasha basin



A visit to one of the ITC stations in Delamare farm (left), and at Paul Ruoya's farm in Kinangop (right)



Different weather in the catchment, evidenced by the muddy roads at downstream areas (left) and dry rocky roads (right)